

Analysis of Digital Clipping and Analog Clipping for OFDM system

Student : Chun-Lin Yang

Advisor : Yuan-Pei Lin

Department of Electrical and Control Engineering
National Chiao Tung University



Abstract

In this thesis, we analyze digital and analog clipping in OFDM system. We derive the equations that show how digital and analog clipping affect the average autocorrelation of the transmitted signal. Earlier analysis of the clipped signals requires the assumption that input signal of the clipper is WSS. However, this assumption is not valid in the OFDM system in practice. We show that the clipper input should adequately be assumed to be WSCS. We will derive the power spectrum of the clipper output. Numerical simulation will be given to demonstrate the transmitted spectrum of the OFDM transmitter using analog clipping spreads more widely than the one using digital clipping. It will also be shown that transmitted spectrum is underestimated if we assume the clipper input signal is WSS.

Contents

1	Introduciton	1
1.1	Outline	3
1.2	Notation	4
1.3	Prerequisite [18]	5
1.3.1	Wide Sense Stationary Process	5
1.3.2	Wide Sense Cyclostationary Process	6
2	A Survey of Previous Works	7
2.1	Analog Representation and DFT-Based Implementation of OFDM Transmitter [17]	7
2.2	Spectral Properties for a Clipped DMT ADSL Signal [16]	8
2.3	DAC with WSS Input Signal [18, 19]	9
3	Advanced Analysis on DAC	11
4	Transmitted Spectrum with Digital Clipping	13
4.1	System Model for Digital Clipping	13
4.2	Statistical Properties of the Modulator Output Signal $y(n)$	15
4.3	Derivation of $\overline{R}_y(k)$	16
4.4	Statistical Properties of the Digital Clipper Output Signal $y_{dc}(n)$	17
4.5	Derivation of $\overline{R}_{y,dc}(k)$	18
4.6	Statistical Properties of the DAC Output Signal $y_{dc}(t)$	18
4.7	Derivation of $\overline{R}_{y,dc}(\tau)$	19

5	Transmitted Spectrum with Analog Clipping	20
5.1	System Model for Analog Clipping	21
5.2	Statistical Properties of the DAC Output Signal $y(t)$ and the Derivation of $\bar{R}_y(\tau)$	22
5.3	Statistical Properties of the Analog Clipper Output Signal $y_{ac}(t)$ and the Derivation of $\bar{R}_{y,ac}(\tau)$	24
6	Numerical Simulation	27
6.1	Spectrums of Analog Representation and DFT-Based Implementation of OFDM Transmitters	27
6.2	Digital Clipping in OFDM system	30
6.3	Analog Clipping in OFDM system	34
6.4	Different Assumption for the Clipper Input Signal	39
7	Conclusion	42
A	Proof of Lemma 1	43
B	Proof of Lemma 2	45
C	Proof of Lemma 3	49
D	Proof of Lemma 5	51
E	Proof of Lemma 6	54
F	Proof of Lemma 7	57
G	Proof of Lemma 8	60
H	Proof of Lemma 16	67



List of Figures

1.1	Analog representation of the OFDM transmitter.	2
1.2	Commonly used DFT-Based implementation of the OFDM transmitter, where $\omega_0 = 2\pi/M$	3
2.1	Schematic diagram of the clipper.	9
2.2	Digital-to-analog conversion scheme.	10
4.1	The OFDM transmitter with a digital clipper.	13
4.2	Equivalent model for digital clipping.	14
4.3	Digital modulator of the M subcarries for one-shot transmission. $w(n)$ is the discrete window of lenth M and $\omega_0 = 2\pi/M$	15
4.4	digital-to-analog converter in the OFDM transmitter with digital clipper.	19
5.1	DFT-Based OFDM transmitter with analog clipper	20
5.2	Equivalent model for DAC.	21
5.3	Equivalent model for analog clipping.	22
6.1	Frequency response of the pulse shaping filter $p(t)$ in Fig. 1.1.	28
6.2	Frequency response of reconstruction filter $h(t)$ in Fig. 1.2.	29
6.3	Average power spectral densities of the output of the two modulation models $x(t)$ and $y(t)$	29
6.4	Average power spectrum of the digital clipper output $\bar{S}_{y,dc}(e^{j\omega})$	31
6.5	Average power spectrum of the OFDM trasnmmitter with digital clipper $\bar{S}_{y,dc}(e^{j\Omega})$. The clipping ratio $A/\sigma_{y_R} = 0.1$	32

6.6	Average power spectrum of the OFDM trasnmitter with digital clipper $\bar{S}_{y,dc}(e^{j\Omega})$. The clipping ratio $A/\sigma_{y_R} = 0.5$	32
6.7	Average power spectrum of the OFDM trasnmitter with digital clipper $\bar{S}_{y,dc}(e^{j\Omega})$. The clipping ratio $A/\sigma_{y_R} = 1$	33
6.8	Average power spectrum of the OFDM trasnmitter with digital clipper $\bar{S}_{y,dc}(e^{j\Omega})$. The clipping ratio $A/\sigma_{y_R} = 3$	33
6.9	Average power spectrum of the OFDM trasnmitter with analog clipper $\bar{S}_{y,ac}(j\Omega)$. The clipping ratio $A/\bar{\sigma}_{y_R} = 0.1$	35
6.10	Average power spectrum of the OFDM trasnmitter with analog clipper $\bar{S}_{y,ac}(j\Omega)$. The clipping ratio $A/\bar{\sigma}_{y_R} = 0.5$	36
6.11	Average power spectrum of the OFDM trasnmitter with analog clipper $\bar{S}_{y,ac}(j\Omega)$. The clipping ratio $A/\bar{\sigma}_{y_R} = 1$	36
6.12	Average power spectrum of the OFDM trasnmitter with analog clipper $\bar{S}_{y,ac}(j\Omega)$. The clipping ratio $A/\bar{\sigma}_{y_R} = 3$	37
6.13	Average power spectrum of the two OFDM trasnmitters with digital and analog clipper, $\bar{S}_{y,dc}(j\Omega)$ and $\bar{S}_{y,ac}(j\Omega)$, respectively. The clipping ratio $A/\sigma_{y_R} = A/\bar{\sigma}_{y_R} = 1$	37
6.14	Average power spectrum of the two OFDM trasnmitters with digital and analog clipper, $\bar{S}_{y,dc}(j\Omega)$ and $\bar{S}_{y,ac}(j\Omega)$, respectively. The clipping ratio $A/\sigma_{y_R} = A/\bar{\sigma}_{y_R} = 3$	38
6.15	Average power spectrum of the two OFDM trasnmitters with digital and analog clipper, $\bar{S}_{y,dc}(j\Omega)$ and $\bar{S}_{y,ac}(j\Omega)$, respectively. The clipping ratio $A/\sigma_{y_R} = A/\bar{\sigma}_{y_R} = 10$	38
6.16	$\bar{S}_{y,ac}(j\Omega)$ with the clipper input under the WSS and WSCS assumption. The clipping ratio $A/\sigma = A/\bar{\sigma}_{y_R} = 0.1$	39
6.17	$\bar{S}_{y,ac}(j\Omega)$ with the clipper input under the WSS and WSCS assumption. The clipping ratio $A/\sigma = A/\bar{\sigma}_{y_R} = 0.5$	40
6.18	$\bar{S}_{y,ac}(j\Omega)$ with the clipper input under the WSS and WSCS assumption. The clipping ratio $A/\sigma = A/\bar{\sigma}_{y_R} = 1$	40
6.19	$\bar{S}_{y,ac}(j\Omega)$ with the clipper input under the WSS and WSCS assumption. The clipping ratio $A/\sigma = A/\bar{\sigma}_{y_R} = 3$	41

Chapter 1

Introduction

Orthogonal frequency-division multiplexing (OFDM) is an attractive transceiver scheme for its high transmission rate for the last several decades [1]-[3]. It has been well-adopted in many practical application, such as radio environment [4], mobile communications [5] and copper wired DSL application [6, 7]. In OFDM, large number of orthogonal subcarriers are used at the transmitter to transmit data, which can be achieved by inverse Discrete Fourier Transform (IDFT). In the similar way, Discrete Fourier Transform (DFT) demodulates the data at the receiver. The IDFT-DFT pair can be implemented by FFT algorithm which reduces the computational complexity. Easily achieved interblock interference (IBI) free is one of the major merits of the OFDM system. By inserting the guard interval, usually known for cyclic prefix (CP), at each block before transmitting, IBI can be removed if the channel order is not greater than the length of CP. Simple equalization is another advantage of the OFDM system. When coping with the frequency-selective channel, each subcarrier can be viewed as suffering a constant scaling if the subcarrier is enough narrow-banded, hence, the receiver needs only one-tap equalization.

One of the disadvantages in utilizing OFDM system is the large peak to average power ratio (PAPR) of the OFDM signal. The large peak at the transmitter will cause the saturation in power amplifier and may suffer from poor power efficiency. Amounts of research have been presented to solve this problem. Several famous solutions such as selective mapping (SLM) [8], which multiplying the

specific sequence to the input signal, or partial transmit sequence (PTS) [9] that dividing the input signal into several subblocks then optimally joint them, they aim the target at how to reduce the probability of generating the large peaks. The drawbacks of these solutions are computational complicated and the side information is necessary.

One popular and convenient method is to clip or limit the peak amplitude of the OFDM signal to a maximum value, called clipping [10]. Clipping is widely used to reduce the large PAPR of the OFDM signals. Unfortunately, it brings the side effect called clipping noise, which is introduced additional out-of-band noise and degrades the performance of the system. Several schemes and investigations have been made to mitigate and analyze the clipping noise [11]-[16]. Though they are broadly adopted, several key problems take place on their modulation scheme and the assumption of the clipper input signal.

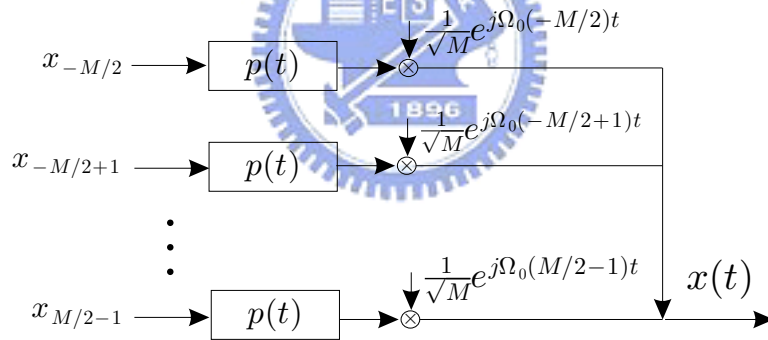


Figure 1.1: Analog representation of the OFDM transmitter.

The transmitter scheme applied in [11]-[14] is shown in Fig. 1.1 and the commonly used digital communication of the OFDM transmitter is shown in Fig. 1.2. $p(t)$ in Fig. 1.1 is the pulse-shaping filter with length $T_0 = 2\pi/\Omega_0$, and $w(n)$ and $h(t)$ are the transmitting window with M taps and reconstruction filter with natural frequency π/T_s , respectively. It is proved that these two kinds of schemes are equivalent only for special choices of $p(t)$, $w(n)$ and $h(t)$ [17] and the spectral roll-off of $x(t)$ and $y(t)$ can be a significant difference. Hence, applying the analog representation model in Fig. 1.1 is not adequate for analyzing the out-of-band

noise.

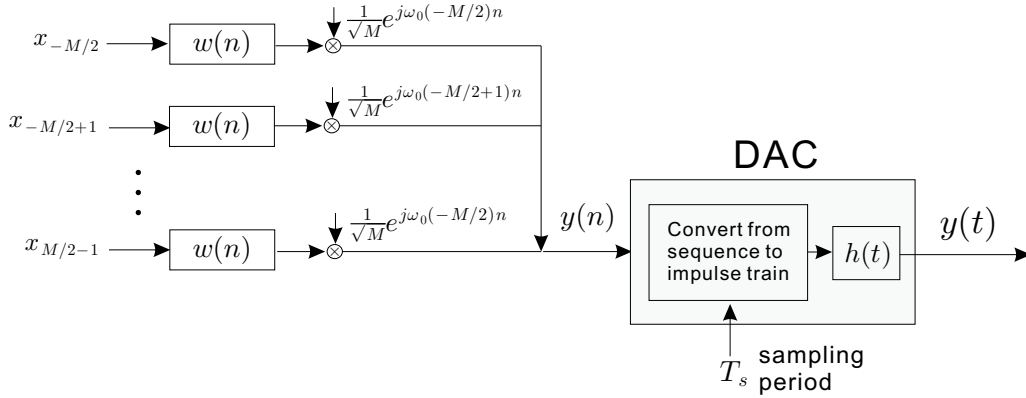


Figure 1.2: Commonly used DFT-Based implementation of the OFDM transmitter, where $\omega_0 = 2\pi/M$

Another major problem is the inappropriate assumption of the clipper input signal. Under the assumption that clipper input is WSS, an analytical research of the clipping noise is given in [11, 16], however, is not appropriate for DFT-Based implementation and will underestimate the effect of the clipping noise.

In this thesis, we consider digital clipping and analog clipping in OFDM system. We begin from the model in Fig. 1.2, then digital or analog clipped are added, respectively. The clipper input $y(t)$ is assumed to be a WSCS process now. In numerical simulation, the difference between the analog representation and DFT-Based implementation of the OFDM transmitter will be shown, especially in spectral roll-off. Also, we will demonstrate that the transmitted spectrum of the analog clipping spreads more widely than the digital clipping ones in different clipping ratio. We will show how that the clipping noise will be underestimated if we assume the clipper input signal is WSS.

1.1 Outline

- Chapter 2: A survey of previous works is given. Including showing the difference between the analog representation and DFT-based implementation

of OFDM transmitter, and the analysis of clipping process under the assumption that clipper input signal is WSS, and illustration of the statistical property of DAC output signal when the DAC input is WSS.

- Chapter 3: Advanced analysis on DAC when DAC input is a WSCS process. A similar result to the case that DAC input is WSS is derived.
- Chapter 4: Each block in the OFDM transmitter with digital clipper is presented. The properties of the OFDM input signal is also introduced. Then, we make the discussions on the statistical properties of the modulator output signal, the digital clipper output signal and the output signal of the DAC. Thereafter, we focus on deriving their average autocorrelation.
- Chapter 5: The OFDM transmitter with analog clipper is shown, such as transmitting window, DAC along with reconstruction filter and analog clipper. Next, the analysis on the statistical properties of the DAC output signal and the output signal of the analog clipper is given. Similarly, this average autocorrelation will be deduced.
- Chapter 6: The simulation will be given in this chapter, including that: Showing the difference in spectral roll-off between the analog representation and DFT-Based implementation of the OFDM transmitter. Comparison of the average spectrum between analog clipping and digital clipping in different clipping ratio. How a different assumption of the clipper input signal affects the estimation of the clipping noise.
- Chapter 7: Conclusion.

1.2 Notation

1. $\Re\{\cdot\}$ denotes taking real part.
2. $\Im\{\cdot\}$ denotes the imaginary part is taken.
3. $*$ denotes convolution.

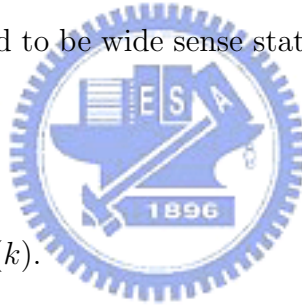
4. $y_R(n)$ represents that the real part of $y(n)$, that is, $\Re\{y(n)\}$.
5. $y_I(n)$ represents that the imaginary part of $y(n)$, that is, $\Im\{y(n)\}$.
6. $\delta(n)$ represents the kronecker delta function.
7. $Q(x)$ is given by $Q(x) = \int_{-\infty}^x e^{-t^2} dt$.
8. The notation $y(n)$ will be abbreviated as y_n when applying mathematical deduction, especially the integration is applied.

1.3 Prerequisite [18]

1.3.1 Wide Sense Stationary Process

A random process $x(n)$ is said to be wide sense stationary(WSS) if $x(n)$ satisfies the following conditions:

1. $E[x(n)] = m_x$,
2. $E[x(n)x^*(n - k)] = R_x(k)$.



Mean function $E[x(n)]$ is a constant independent of n and the autocorrelation function $E[x(n)x^*(n - k)]$ depends on time difference k , not n . We define the power spectrum of a WSS process as the Fourier transform of the autocorrelation function $R_x(k)$,

$$S_x(e^{j\omega}) \triangleq \sum_{k=-\infty}^{\infty} R_x(k)e^{-j\omega k}.$$

For continuous time random processes, WSS property can be define in a similar manner. We say a continuous time random process $y(t)$ is WSS if the mean function $E[y(t)]$ is independent of t and the autocorrelation function $E[y(t)y^*(t - \tau)]$ only depends on τ . The power spectrum of a WSS process is defined as the Fourier transform of the autocorrelation function,

$$S_y(j\Omega) \triangleq \int_{-\infty}^{\infty} R_y(\tau)e^{-j\Omega\tau} d\tau.$$

1.3.2 Wide Sense Cyclostationary Process

A random process $x(n)$ is said to be wide sense cyclostationary with period M (denoted by WSCS(M)) if it satisfies the following conditions:

1. $E[x(n)] = E[x(n + M)],$
2. $E[x(n)x^*(n - k)] = E[x(n + M)x^*(n + M - k)].$

These two properties represents that mean function $E[x(n)]$ and the autocorrelation function $E[x(n)x^*(n - k)]$ is a periodic function of n with period M . We define the average autocorrelation function as

$$\bar{R}_x(k) \triangleq \frac{1}{M} \sum_{n=0}^{M-1} E[x(n)x^*(n - k)].$$

Also, we define the average power spectrum of a WSCS process as the Fourier transform of the average autocorrelation function,

$$\bar{S}_x(e^{j\omega}) \triangleq \sum_{k=-\infty}^{\infty} \bar{R}_x(k)e^{-j\omega k}.$$

Similarly, we can define wide sense cyclostationary property for continuous time random process. We say a continuous time random process $y(t)$ is wide sense cyclostationary with period T (denoted by WSCS(T)) if

1. $E[y(t)] = E[y(t + T)],$
2. $E[y(t)y^*(t - \tau)] = E[y(t + T)y^*(t + T - \tau)].$

Mean function $E[y(t)]$ and the autocorrelation function $E[y(t)y^*(t - \tau)]$ is a periodic function of t with period T . The average autocorrelation function is defined as

$$\bar{R}_y(\tau) \triangleq \frac{1}{T_s} \int_0^{T_s} E[y(t)y^*(t - \tau)]dt.$$

Then we define the average power spectrum of a WSCS process as the Fourier transform of the average autocorrelation function,

$$\bar{S}_y(j\Omega) \triangleq \int_{-\infty}^{\infty} \bar{R}_y(\tau)e^{-j\Omega\tau} d\tau.$$

Chapter 2

A Survey of Previous Works

In this Chapter, we will introduce earlier analysis on analog and digital modulation process, clipping scheme and digital-to-analog conversion.

2.1 Analog Representation and DFT-Based Implementation of OFDM Transmitter [17]

In this section, we reviewed the results relates to the analog and digital modulator, the explicit derivations are stated in [17].

Theorem 1 : Let the OFDM transmitter in Fig. 1.2 have a rectangular window $w(n)$

$$w(n) = \begin{cases} 1, & 0 \leq n \leq M - 1 \\ 0, & \text{otherwise} \end{cases}$$

and an ideal lowpass reconstruction filter $h(t)$ with

$$H(j\Omega) = \begin{cases} 1, & |\Omega| < \frac{\pi}{T_s} \\ 0, & \text{otherwise.} \end{cases}$$

The outputs of the two systems, respectively, $x(t)$ in Fig. 1.1 and $y(t)$ in Fig. 1.2, are not the same for any choice of pulse shaping filter $p(t)$.

Theorem 2 : The analog OFDM transmitter in Fig. 1.1 with a rectangular pulse $p(t)$ does not admit the DFT-based implementation in Fig. 1.2, regardless of the choices of $w(n)$ and $h(t)$.

Above two theorems state that for commonly used digital window, reconstruction filter and pulse shaping filter, the analog representation and DFT-based implementation of OFDM transmitter are not equivalent. The following theorem will show that these two transmitters are equivalent for only special cases.

Theorem 3 : *The OFDM transmitter in Fig. 1.1 can be implemented as in Fig. 1.2, namely, the two systems are equivalent, if and only if the pulse shaping filter $p(t)$, the digital window $w(n)$, and the reconstruction filter $h(t)$ satisfy*

$$W(e^{j\Omega T_s})H(j(\Omega + k\Omega_0)) = G(j\Omega), \text{ for } k = -M/2, -M/2 + 1, \dots, M/2 - 1.$$

2.2 Spectral Properties for a Clipped DMT ADSL Signal [16]

In this section, the analysis relates to the clipper is reviewed. The schematic diagram of the clipper is shown in Fig. 2.1. The clipper input signal $x(t)$ is a DMT signal consists of a sum of modulated sinusoids which can be represented as a zero mean Gaussian random process. In addition, $x(t)$ is assumed to be WSS with variance σ^2 . The clipping can be modeled by a clipping function $g(\cdot)$ as follows

$$y(t) = g(x(t)) = \begin{cases} A, & x(t) \geq A \\ x(t), & -A < x(t) < A \\ -A, & x(t) \leq -A \end{cases} .$$

The statistics of the clipper output signal $y(t)$ is developed in [16], which will be stated in the following theorem. The explicit derivations are also given in [16].

Theorem 4 : *If the clipper input signal $x(t)$ is a WSS, zero mean Gaussian random process with variance σ^2 , and we suppose the autocorrelation function of $x(t)$ is $R_x(\tau)$, where $R_x(0) = \sigma^2$, then the autocorrelation function of the clipper output $y(t)$ can be expressed as*

$$R_y(\tau) = R_x(0) \left[\text{erf}^2 \left(\frac{A}{\sqrt{2}\sigma} \right) r(\tau) + \sum_{n=2,4,\dots}^{\infty} C_n [r(\tau)]^{n+1} \right]$$

where $r(\tau) = R_x(\tau)/R_x(0)$, $\text{erf}(\cdot)$ denotes the error function, the sum over the index n is for even numbers only, and the distortion coefficients C_n is

$$C_n = \frac{4H_{n-1}^2\left(\frac{A}{\sqrt{2}\sigma}\right)}{\pi 2^n (n+1)!} \cdot \exp\left\{\frac{-A^2}{\sigma^2}\right\}$$

with H_n a Hermite polynomial of order n .

Notice that the first term of $R_y(\tau)$ is usually called in-band signal which relates to the spectrum of the clipper input signal $x(t)$, and the second term often named as clipping noise which comes from the clipping process and distorts the spectrum of clipper input signal.

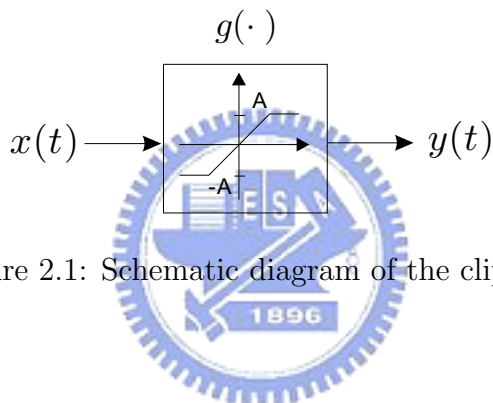


Figure 2.1: Schematic diagram of the clipper.

2.3 DAC with WSS Input Signal [18, 19]

We will introduce previous investigations on a WSS signal passing through DAC in this section. The DAC scheme is shown in Fig. 2.2. The DAC input signal $x(n)$ is a WSS random process, $p_1(t)$ is the reconstruction filter and the sampling period of DAC is T . We will demonstrate that the DAC output signal $x(t)$ becomes a WSCS process and give the expression of the average autocorrelation and average power spectrum of $x(t)$. The explicit derivations have been shown in [18, 19].

Theorem 5 : Consider the DAC with a reconstruction filter $p_1(t)$ and sampling period T as shown in Fig. 2.2. When the input signal $x(n)$ is WSS, the output $x(t)$ is a continuous time WSCS(T) process, that is,

$$E[x(t)] = E[x(t+T)], \quad E[x(t)x^*(t-\tau)] = E[x(t+T)x^*(t+T-\tau)].$$

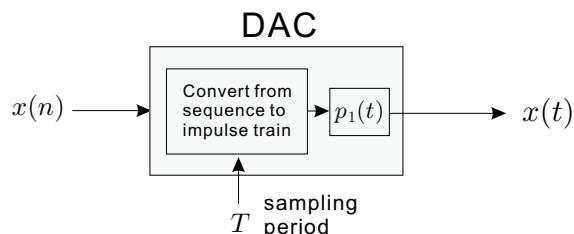


Figure 2.2: Digital-to-analog conversion scheme.

Theorem 6 : When the input signal of DAC $x(n)$ in Fig. 2.2 is WSS, the output WSCS(T) random process $x(t)$ has an average autocorrelation

$$\bar{R}_x(\tau) = \frac{1}{T} \sum_{k=-\infty}^{\infty} R_x(k) f(\tau - kT)$$

where

$$\bar{R}_x(\tau) \triangleq \frac{1}{T} \int_0^T E[x(t)x^*(t - \tau)] dt$$

and

$$R_x(k) = E[x(n)x^*(n - k)].$$

Then function $f(\tau)$ is defined as

$$\begin{aligned} f(\tau) &\triangleq p_1(\tau) * p_1(-\tau) \\ &= \int_{-\infty}^{\infty} p_1(t)p_1(t - \tau) dt \end{aligned}$$

where $*$ denotes convolution.

Taking the Fourier transform of the above conclusion, we obtain the average power spectrum of $x(t)$ as

$$S_x(j\Omega) = \frac{1}{T} S_x(e^{j\Omega T}) |P_1(j\Omega)|^2,$$

where $P_1(j\Omega)$ is the Fourier transform of the reconstruction filter $p_1(t)$.

Chapter 3

Advanced Analysis on DAC

In section 2.3, we demonstrate the autocorrelation of the output signal of DAC when the input signal is a WSS process. We now make an investigation on the DAC output signal $x(t)$ in Fig. 2.2 while the input signal $x(n)$ is a WSCS process.

The following lemma will show that DAC output signal $x(t)$ is still a WSCS process even the DAC input signal turns into a WSCS process.

Lemma 1 : *If the DAC input $x(n)$ in Fig. 2.2 is a WSCS(M) process, then the DAC output $x(t)$ in Fig. 2.2 is a WSCS(MT) process, where T is the sampling period of DAC.*

Proof: The explicit derivation will be given in Appendix A. △△△

Next, we will demonstrate the average autocorrelation of the DAC output signal $x(t)$, it can be seen that the expression is almost the same as the case that DAC input signal is a WSS process.

Lemma 2 : *When the input signal of DAC $x(n)$ in Fig. 2.2 is WSCS(M), the output WSCS(MT) random process $x(t)$ has an average autocorrelation*

$$\bar{R}_x(\tau) = \frac{1}{T} \sum_{k=-\infty}^{\infty} \bar{R}_x(k) f(\tau - kT), \quad (3.1)$$

where

$$\bar{R}_x(\tau) \triangleq \frac{1}{MT} \int_0^{MT} E[x(t)x^*(t - \tau)] dt \quad (3.2)$$

and

$$\bar{R}_x(k) = \frac{1}{M} \sum_{n=0}^{M-1} E[x(n)x^*(n - k)]. \quad (3.3)$$

Then function $f(\tau)$ in (3.1) is defined as

$$\begin{aligned} f(\tau) &\triangleq p_1(\tau) * p_1(-\tau) \\ &= \int_{-\infty}^{\infty} p_1(t)p_1(t - \tau)dt \end{aligned} \tag{3.4}$$

where $*$ denotes convolution.

Proof: The derivation will be completely shown in Appendix B. $\triangle\triangle\triangle$



Chapter 4

Transmitted Spectrum with Digital Clipping

We aim our target at deriving $\bar{R}_{y,dc}(\tau)$ in this chapter. That is, we wish to derive the average autocorrelation of the signal $y_{dc}(t)$ in Fig. 4.1. Hence, the statistical properties of each output signal $y(n)$, $y_{dc}(n)$, and $y_{dc}(t)$ in Fig. 4.1 should be discussed, and then the average autocorrelation $\bar{R}_y(k)$, $\bar{R}_{y,dc}(k)$, and $\bar{R}_{y,dc}(\tau)$ can be derived correspondingly.

4.1 System Model for Digital Clipping

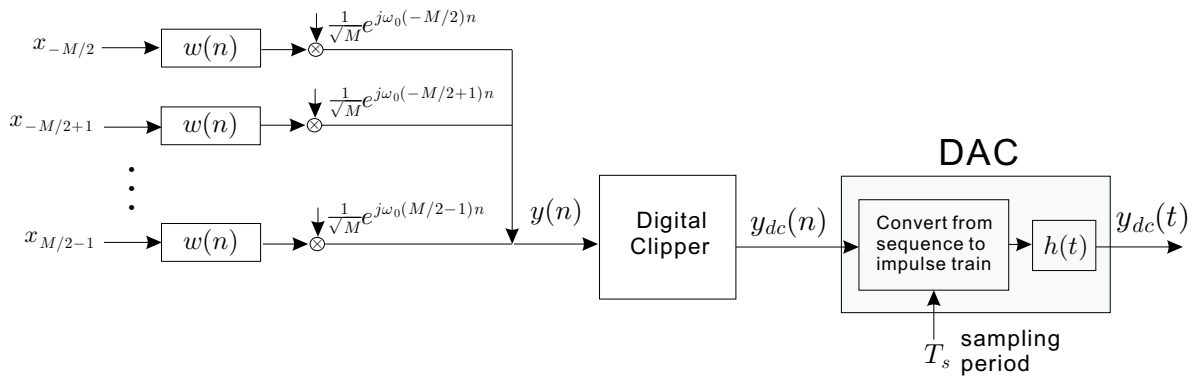


Figure 4.1: The OFDM transmitter with a digital clipper.

In this section, the system model used for digital clipping is presented. Fig. 4.1 is the commonly used DFT-Based OFDM transmitter with a digital clipper. The

first part performs the digital modulation of the M subcarriers with frequency spacing $\omega_0 = 2\pi/M$. The scalar $\frac{1}{\sqrt{M}}$ is the normalized scaling. The input sequence of the OFDM system x_k is a white, Gaussian distributed random process with zero mean and variance σ_x^2 . $w(n)$ is a discrete window with real coefficients of length M . After digital modulating, $y(n)$ is the modulator output as indicated in Fig. 4.1.

The second part carrying out the digital clipping. The digital clipper limits the real part of the clipper input sequence $y_R(n)$ and imaginary part of the clipper input sequence $y_I(n)$ separately. The output signals of the limiting processes are $y_{dc,R}(n)$ and $y_{dc,I}(n)$, respectively. Combining both outputs sequence results in the digital clipper output sequence $y_{dc}(n)$. The clipping process can be equivalently modeled by two individual and identical clipping functions $g(\cdot)$ shown in Fig. 4.2. The clipping function $g(\cdot)$ is defined as

$$y = g(x) = \begin{cases} A, & x \geq A \\ x, & -A < x < A \\ -A, & x \leq -A \end{cases} . \quad (4.1)$$

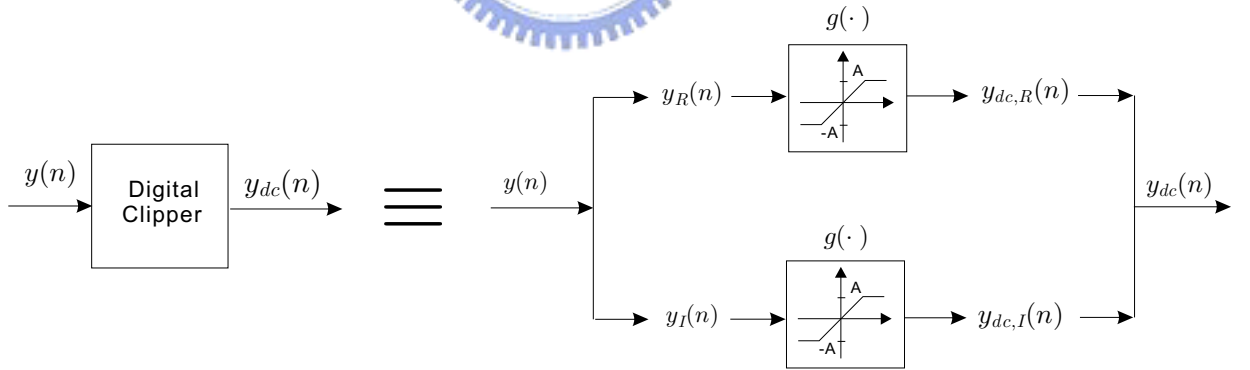


Figure 4.2: Equivalent model for digital clipping.

The last part of the OFDM transmitter with the digital clipper performs a digital-to-analog conversion, which converting the sequence to the impulse train, then passing through the reconstruction filter $h(t)$ and the output signal $y_{dc}(t)$ is generated eventually . A reconstruction filter is usually a lowpass filter with real coefficients. Notice that the sampling period of the DAC is T_s .

4.2 Statistical Properties of the Modulator Output Signal $y(n)$

In this section, we analyze the statistical properties of the modulator output signal $y(n)$, including showing that $y(n)$ is a WSCS process, and with jointly Gaussian distributed.

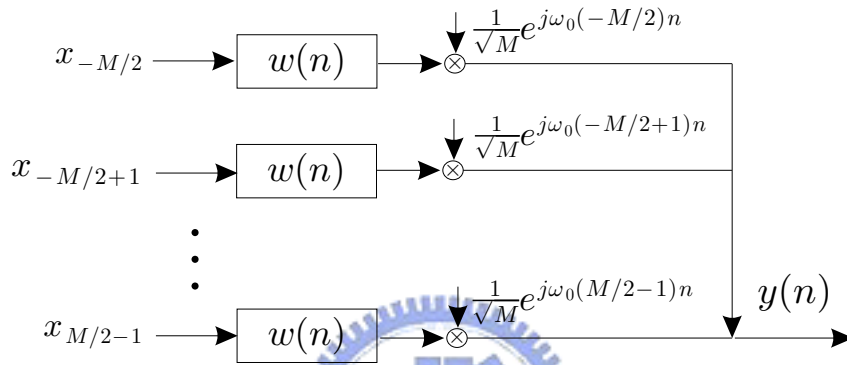


Figure 4.3: Digital modulator of the M subcarries for one-shot transmission. $w(n)$ is the discrete window of length M and $\omega_0 = 2\pi/M$

The output of the modulator $y(n)$ in Fig. 4.3 is given by

$$y(n) = w(n) \cdot \frac{1}{\sqrt{M}} \sum_{k=-\frac{M}{2}}^{\frac{M}{2}-1} x_{k+B(n)M} \cdot e^{j\frac{2\pi}{M}kn}, \quad \forall n \in \mathbb{Z} \quad (4.2)$$

where $w(n)$ is the transmitting window with M coefficients, $B(n) = \lfloor \frac{n}{M} \rfloor$ is the block indicator. x_k can be expressed as $a_k + jb_k$, where a_k and b_k can be reasonably assumed that

$$\begin{aligned} E[a_l a_m] &= E[b_l b_m] = \frac{1}{2} \sigma_x^2 \delta(l - m) \\ E[a_l b_m] &= 0 \end{aligned} \quad \forall l, m \in \mathbb{Z}. \quad (4.3)$$

Firstly, it can be shown that $y(n)$ is a WSCS process under the assumption that x_k is a white process.

Lemma 3 : *If the input of the OFDM system x_k is a white process, then the output of the modulator $y(n)$ in Fig. 4.3 is WSCS. Especially, if the M point IDFT*

is used, then $y(n)$ is a WSCS process with period M , denoted as $WSCS(M)$

Proof: The explicit derivation will be given in Appendix C. △△△

Secondly, we demonstrate the proof that $y(n)$ is a jointly Gaussian random process.

Lemma 4 : If x_k is a jointly Gaussian random process, then $y(n)$ in Fig. 4.3 is also a jointly Gaussian random process.

Proof: Since $y(n) = w(n) \cdot \frac{1}{\sqrt{M}} \sum_{k=-\frac{M}{2}}^{\frac{M}{2}-1} x_{k+B(n)M} \cdot e^{j\frac{2\pi}{M}kn}$, which is a linear combination of x_k , therefore indeed a jointly Gaussian distributed random process. △△△

4.3 Derivation of $\bar{R}_y(k)$

We now derive $\bar{R}_y(k)$, which is the average autocorrelation of $y(n)$ in Fig. 4.3.

Lemma 5 : $y(n) = w(n) \cdot \frac{1}{\sqrt{M}} \sum_{k=-\frac{M}{2}}^{\frac{M}{2}-1} x_{k+B(n)M} \cdot e^{j\frac{2\pi}{M}kn} \triangleq y_R(n) + jy_I(n)$, where $y_R(n) = \Re\{y(n)\}$ and $y_I(n) = \Im\{y(n)\}$. It can be shown that

1. $y_R(n)$ and $y_I(n)$ are uncorrelated, that is, $E[y_R(n)y_I(m)] = 0, \forall n, m \in \mathbb{Z}$.
2. The joint pdf $f(y_{R,n}, y_{R,m}, y_{I,n}, y_{I,m})$ can be separated as

$$f(y_{R,n}, y_{R,m}, y_{I,n}, y_{I,m}) = f(y_{R,n}, y_{R,m}) \cdot f(y_{I,n}, y_{I,m})$$

3. $E[y_R(n)y_R(m)] = E[y_I(n)y_I(m)] = \frac{1}{2}\sigma_x^2 w(n)w(m)\delta(m-n)$.
4. $\bar{R}_y(k) = \bar{R}_{y,R}(k) + \bar{R}_{y,I}(k) = \frac{1}{M} \sum_{n=0}^{M-1} \sigma_x^2 w(n)w(n-k)\delta(k)$.

where $\bar{R}_y(k)$ is defined as

$$\bar{R}_y(k) = \frac{1}{M} \sum_{n=0}^{M-1} E[y(n)y^*(n-k)]$$

, which is a function independent of n .

Proof: The derivation is demonstrated in Appendix D. △△△

4.4 Statistical Properties of the Digital Clipper Output Signal $y_{dc}(n)$

In this section, we discuss the statistical properties of the clipper output signal $y_{dc}(n)$ in Fig. 4.2, including giving the proof that $y_{dc,R}(n)$ and $y_{dc,I}(n)$ are uncorrelated and showing that $y_{dc}(n)$ is also a WSCS process.

Lemma 6 : *If the joint pdf $f(y_{R,n}, y_{R,n-k}, y_{I,n}, y_{I,n-k}) = f(y_{R,n}, y_{R,n-k}) \cdot f(y_{I,n}, y_{I,n-k})$, then the real and imaginary part in the output of the digital clipper, $y_{dc,R}(n)$ and $y_{dc,I}(n)$ in Fig. 4.2, should be uncorrelated. Accordingly, we have*

$$E[y_{dc}(n)y_{dc}^*(n-k)] = E[y_{dc,R}(n)y_{dc,R}(n-k)] + E[y_{dc,I}(n)y_{dc,I}(n-k)].$$

Then obviously,

$$\bar{R}_{y,dc}(k) = \bar{R}_{y,dc,R}(k) + \bar{R}_{y,dc,I}(k).$$

Notice that

$$y_{dc,R}(n) = g(y_R(n))$$

$$y_{dc,I}(n) = g(y_I(n))$$

$$\bar{R}_{y,dc}(k) = \frac{1}{M} \sum_{n=0}^{M-1} E[y_{dc}(n)y_{dc}^*(n-k)]$$

$$\bar{R}_{y,dc,R}(k) = \frac{1}{M} \sum_{n=0}^{M-1} E[y_{dc,R}(n)y_{dc,R}(n-k)].$$

$$\bar{R}_{y,dc,I}(k) = \frac{1}{M} \sum_{n=0}^{M-1} E[y_{dc,I}(n)y_{dc,I}(n-k)].$$

Proof: The derivation will be given in Appendix E. △△△

Lemma 7 : *If the input sequence of the digital clipper $y(n)$ is a Gaussian distributed WSCS(M) process, then the output sequence of the digital clipper $y_{dc}(n)$ is also WSCS(M).*

Proof: The derivation will be presented in Appendix F. △△△

4.5 Derivation of $\overline{R}_{y,dc}(k)$

We then focus on the relationship between the input and the output of the digital clipper, i.e., $y(n)$ and $y_{dc}(n)$ in Fig. 4.2, especially the relationship of the average autocorrelation. We then give the explicit derivation of $\overline{R}_{y,dc}(k)$.

Lemma 8 : *If the digital clipper input signal $y(n)$ is WSCS, then $\overline{R}_{y,dc}(k)$, the average autocorrelation of clipper output signal $y_{dc}(n)$, can be expressed as*

$$\begin{aligned} \overline{R}_{y,dc}(k) &= \frac{2}{M} \sum_{n=0}^{M-1} \operatorname{erf}\left(\frac{A}{\sqrt{2}\sigma_{y_{R,n}}}\right) \operatorname{erf}\left(\frac{A}{\sqrt{2}\sigma_{y_{R,n-k}}}\right) E[y_{R,n}y_{R,n-k}] \\ &\quad + \frac{2}{M} \sum_{n=0}^{M-1} \sum_{m=2,4,\dots}^{\infty} D_m E^{m+1}[y_{R,n}y_{R,n-k}] \end{aligned}$$

where

$$D_m = \frac{4H_{m-1}\left(\frac{A}{\sqrt{2}\sigma_{y_{R,n}}}\right)H_{m-1}\left(\frac{A}{\sqrt{2}\sigma_{y_{R,n-k}}}\right)}{\pi \cdot 2^m \cdot (m+1)! \cdot \sigma_{y_{R,n}}^m \cdot \sigma_{y_{R,n-k}}^m} \exp\left(-\frac{A^2}{2\sigma_{y_{R,n}}^2}\right) \exp\left(-\frac{A^2}{2\sigma_{y_{R,n-k}}^2}\right).$$

Proof: The explicit derivation will be given in Appendix G. △△△

4.6 Statistical Properties of the DAC Output Signal $y_{dc}(t)$

We have shown the equation of $\overline{R}_{y,dc}(k)$, which is the average autocorrelation of the input signal of DAC $y_{dc}(n)$. In this section, we are going to make an analysis on the statistical properties of the DAC output signal $y_{dc}(t)$. We are going to show that the output of DAC $y_{dc}(t)$ is also a WSCS process, then the derivation average autocorrelation of the DAC output $\overline{R}_{y,dc}(\tau)$ would be stated in next section.

Lemma 9 : *If the DAC input $y_{dc}(n)$ in Fig. 4.4 is a WSCS(M) sequence, then the DAC output $y_{dc}(t)$ in Fig. 4.4 is a WSCS(MT_s) process, where T_s is the sampling period of DAC.*

Proof: The conclusion can be directly derived from Lemma 1. △△△

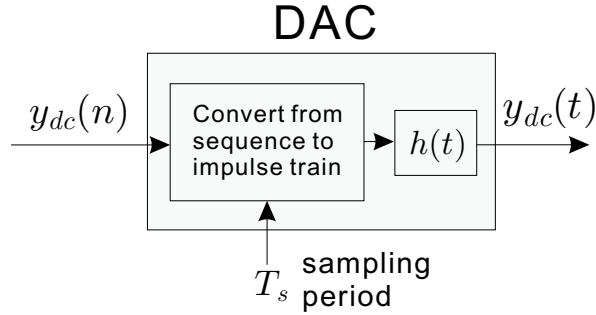


Figure 4.4: digital-to-analog converter in the OFDM transmitter with digital clipper.

4.7 Derivation of $\bar{R}_{y,dc}(\tau)$

We then derive $\bar{R}_{y,dc}(\tau)$, the average autocorrelation of $y_{dc}(t)$ in Fig. 4.4.

Lemma 10 : If $y_{dc}(n)$ in Fig. 4.4 is a WSCS(M) sequence and $y_{dc}(t)$ is the output signal that $y_{dc}(n)$ passing through the DAC in Fig. 4.4, then

$$\bar{R}_{y,dc}(\tau) = \frac{1}{T_s} \sum_{k=-\infty}^{\infty} \bar{R}_{y,dc}(k) f(\tau - kT_s), \quad (4.4)$$

where

$$\bar{R}_{y,dc}(\tau) \triangleq \frac{1}{MT_s} \int_0^{MT_s} E[y_{dc}(t)y_{dc}^*(t-\tau)]dt \quad (4.5)$$

and

$$\bar{R}_{y,dc}(k) = \frac{1}{M} \sum_{n=0}^{M-1} E[y_{dc}(n)y_{dc}^*(n-k)]. \quad (4.6)$$

$f(\tau)$ is defined as

$$\begin{aligned} f(\tau) &\triangleq h(\tau) * h(-\tau) \\ &= \int_{-\infty}^{\infty} h(t)h(t-\tau)dt \end{aligned} \quad (4.7)$$

where $*$ denotes convolution.

Proof: The conclusion can be apparently made from Lemma 2. △△△

Chapter 5

Transmitted Spectrum with Analog Clipping

In this chapter, our focus is to derive $\bar{R}_{y,ac}(\tau)$, i.e., to derive the average autocorrelation of the signal $y_{ac}(t)$ in Fig. 5.1. Hence, the statistical properties of the each output signal $y(n)$, $y(t)$ and $y_{ac}(t)$ in Fig. 5.1 should be discussed, then the average autocorrelation $\bar{R}_y(k)$, $\bar{R}_y(\tau)$ and $\bar{R}_{y,ac}(\tau)$ are able to be derived correspondingly. However, we have investigated the properties $y(n)$ and derived the representation of $\bar{R}_y(k)$ in chapter 4, therefore, the following paragraph will be concentrated on the statistical properties of $y(t)$, $y_{ac}(t)$ and the derivation of $\bar{R}_y(\tau)$ and $\bar{R}_{y,ac}(\tau)$.

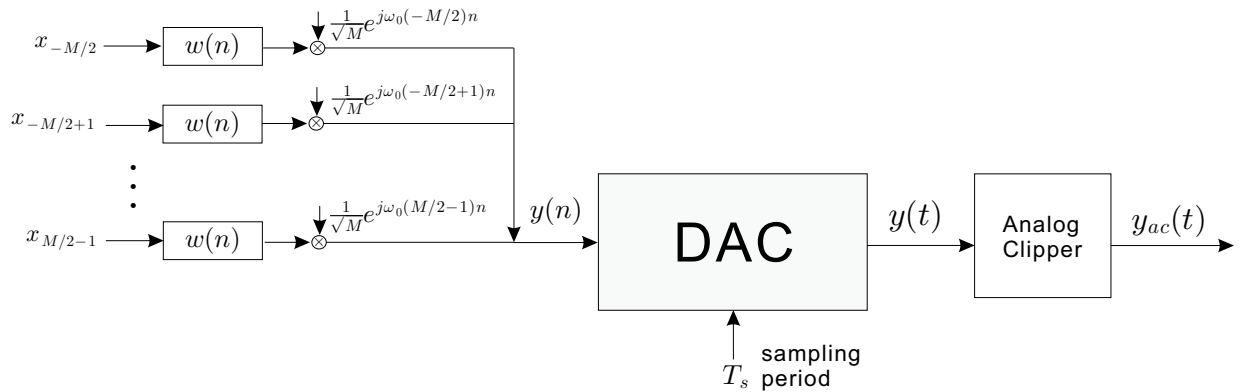


Figure 5.1: DFT-Based OFDM transmitter with analog clipper

5.1 System Model for Analog Clipping

In this section, the system model used for analog clipping is presented. Fig. 5.1 is the commonly used DFT-Based OFDM transmitter with analog clipper. Similar to the structure in Fig. 4.1, the first part performs the digital modulation of the M subcarriers with frequency spacing $\omega_0 = 2\pi/M$. The assumption of x_k and the parameters of $w(n)$ are the same as those in Fig. 4.1. $y(n)$ is also the modulator output as indicated in Fig. 5.1.

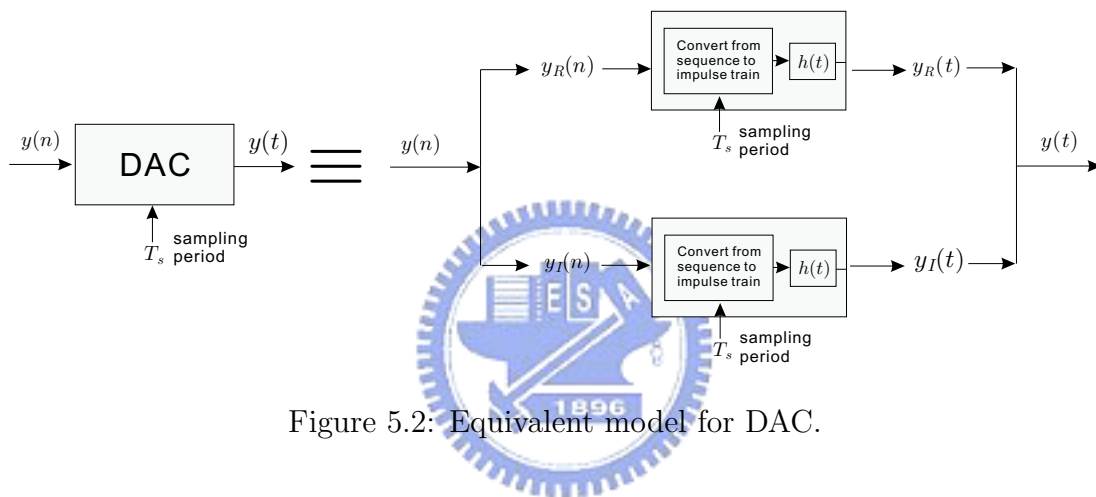


Figure 5.2: Equivalent model for DAC.

The second part carrying out the digital-to-analog converting now. The structure of the DAC is shown in Fig. 5.2, which applying digital-to-analog conversion individually on both the real part and imaginary part of the input signal, $y_R(n)$ and $y_I(n)$. And the output signal of the DAC $y(t)$ is the combination of the output of the converted signal $y_R(t)$ and $y_I(t)$. The reconstruction filter $h(t)$ and the sampling period T_s is the same as what we presented in section 4.1.

The last part is the analog clipper. It is similar that analog clipper limits the real part of the clipper input signal $y_R(t)$ and imaginary part of the clipper input sequence $y_I(t)$ separately. The output signal of the process are $y_{ac,R}(t)$ and $y_{ac,I}(t)$, respectively. The output of the analog clipper $y_{ac}(t)$ is the combination of $y_{ac,R}(t)$ and $y_{ac,I}(t)$. The clipping process can also be equivalently modeled by two individual and identical clipping functions $g(\cdot)$ shown in Fig. 5.3. The clipping function $g(\cdot)$ is defined in (4.1).

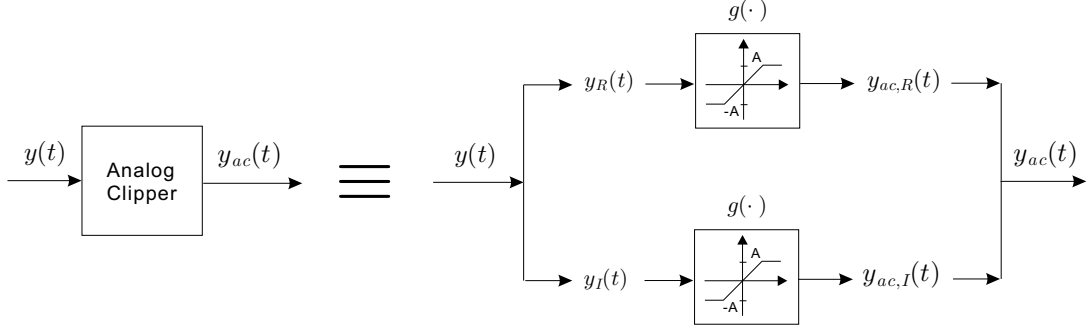


Figure 5.3: Equivalent model for analog clipping.

5.2 Statistical Properties of the DAC Output Signal $y(t)$ and the Derivation of $\overline{R}_y(\tau)$

In this section, the analysis on the statistical properties of the DAC output signal $y(t)$ in Fig. 5.2 is given. We are going to show that: $y_R(t)$ and $y_I(t)$ are uncorrelated, $y(t)$ is a Gaussian WSCS process, the joint pdf $f(y_{R,t}, y_{R,t-\tau}, y_{I,t}, y_{I,t-\tau}) = f(y_{R,t}, y_{R,t-\tau}) \cdot f(y_{I,t}, y_{I,t-\tau})$. Then, the derivation on the average autocorrelation of the DAC output $\overline{R}_y(\tau)$ are also to be shown in this section.

Lemma 11 : *The real part and the imaginary part of the DAC output in Fig. 5.2, $y_R(t)$ and $y_I(t)$, are uncorrelated. Thus,*

$$E[y(t)y^*(t - \tau)] = E[y_R(t)y_R(t - \tau)] + E[y_I(t)y_I(t - \tau)].$$

Proof: From Fig. 5.2, we have

$$\begin{aligned} y_R(t) &= \sum_{n=-\infty}^{\infty} y_R(n)h(t - nT_s) \\ y_I(t - \tau) &= \sum_{m=-\infty}^{\infty} y_I(m)h(t - \tau - mT_s). \end{aligned} \quad (5.1)$$

And their cross correlation will be

$$E[y_R(t)y_I(t - \tau)] = \sum_{n=-\infty}^{\infty} \sum_{m=-\infty}^{\infty} E[y_R(n)y_I(m)]h(t - nT_s)h(t - \tau - mT_s). \quad (5.2)$$

From Lemma 5, we know that $E[y_R(n)y_I(m)] = 0$, therefore, we have the first conclusion that $E[y_R(t)y_I(t - \tau)] = 0, \forall \tau \in \mathbb{R}$.

Therefore, the autocorrelation of $y(t)$ becomes

$$\begin{aligned} E[y(t)y^*(t - \tau)] &= E\left[\left(y_R(t) + jy_I(t)\right)\left(y_R(t - \tau) - jy_I(t - \tau)\right)\right] \\ &= E[y_R(t)y_R(t - \tau)] + E[y_I(t)y_I(t - \tau)]. \end{aligned} \quad (5.3)$$

We have given the proof of all the statement. △△△

We are going to demonstrate the proof that $y(t)$ is a jointly Gaussian process and independence of the joint pdf.

Lemma 12 : *The DAC output $y(t)$ in Fig. 5.2 is a jointly Gaussian process and the joint pdf*

$$f(y_{R,t}, y_{R,t-\tau}, y_{I,t}, y_{I,t-\tau}) = f(y_{R,t}, y_{R,t-\tau}) \cdot f(y_{I,t}, y_{I,t-\tau}).$$

Proof: From Fig. 5.2, we have

$$\begin{aligned} y(t) &= y_R(t) + jy_I(t) \\ &= \sum_{n=-\infty}^{\infty} \left(y_R(n) + jy_I(n)\right)h(t - nT_s). \end{aligned} \quad (5.4)$$

Since $y_R(n)$ and $y_I(n)$ are both jointly Gaussian distributed, therefore, $y(t)$ is a linear combination of $y_R(n)$ and $y_I(n)$, which is a jointly Gaussian process. This is the demonstration of the first statement. And from Lemma 11, we know that

$$E[y_R(t)y_I(t - \tau)] = 0, \quad \forall \tau \in \mathbb{R}. \quad (5.5)$$

Hence, the joint pdf $f(y_{R,t}, y_{R,t-\tau}, y_{I,t}, y_{I,t-\tau})$ apparently turns into

$$f(y_{R,t}, y_{R,t-\tau}, y_{I,t}, y_{I,t-\tau}) = f(y_{R,t}, y_{R,t-\tau}) \cdot f(y_{I,t}, y_{I,t-\tau}). \quad (5.6)$$

△△△

Next, the proof the $y(t)$ is a WSCS process is given. In fact, the following proof is based on the former deduction results.

Lemma 13 : The DAC output $y(t)$ in Fig. 5.2 is a WSCS process with period MT_s .

Proof: This result is a direct conclusion from Lemma 1. △△△

Now, the final paragraph of this section is to show the average autocorrelation $\bar{R}_y(\tau)$. The derivation is also based on the results in Chapter 3.

Lemma 14 : If $y(n)$ is a WSCS(M) process and $y(t)$ is the output signal that $y(n)$ passing through the DAC in Fig. 5.2, then

$$\bar{R}_y(\tau) = \frac{1}{T_s} \sum_{k=-\infty}^{\infty} \bar{R}_y(k) f(\tau - kT_s), \quad (5.7)$$

where

$$\bar{R}_y(\tau) \triangleq \frac{1}{MT_s} \int_0^{MT_s} E[y(t)y^*(t - \tau)] dt, \quad (5.8)$$

$$\bar{R}_y(k) = \frac{1}{M} \sum_{n=0}^{M-1} E[y(n)y^*(n - k)], \quad (5.9)$$

and $f(\tau)$ is defined as

$$\begin{aligned} f(\tau) &\triangleq h(\tau) * h(-\tau) \\ &= \int_{-\infty}^{\infty} h(t)h(t - \tau) dt, \end{aligned} \quad (5.10)$$

where $*$ denotes convolution.

Proof: It is an apparent conclusion can be made from Lemma 2. △△△

5.3 Statistical Properties of the Analog Clipper Output Signal $y_{ac}(t)$ and the Derivation of $\bar{R}_{y,ac}(\tau)$

In this section, firstly we will show the statistical properties of the analog clipper output signal $y_{ac}(t)$, more explicitly, to prove that $E[y_{ac,R}(t)y_{ac,I}(t)] = 0, \forall t \in \mathbb{R}$. Then, the derivation of $\bar{R}_{y,ac}(\tau)$ will be given.

Lemma 15 : If the joint pdf $f(y_{R,t}, y_{R,t-\tau}, y_{I,t}, y_{I,t-\tau}) = f(y_{R,t}, y_{R,t-\tau}) \cdot f(y_{I,t}, y_{I,t-\tau})$, then the real and imaginary part in the output of the digital clipper, $y_{ac,R}(t)$ and

$y_{ac,I}(t)$ in Fig. 5.3, should be uncorrelated. Accordingly, we have

$$E[y_{ac}(t)y_{ac}^*(t-\tau)] = E[y_{ac,R}(t)y_{ac,R}(t-\tau)] + E[y_{ac,I}(t)y_{ac,I}(t-\tau)].$$

Then obviously,

$$\overline{R}_{y,ac}(\tau) = \overline{R}_{y,ac,R}(\tau) + \overline{R}_{y,ac,I}(\tau).$$

Notice that

$$y_{ac,R}(t) = g(y_R(t))$$

$$y_{ac,I}(t) = g(y_I(t))$$

$$\overline{R}_{y,ac}(\tau) = \frac{1}{MT_s} \int_0^{MT_s} E[y_{ac}(t)y_{ac}^*(t-\tau)]dt$$

$$\overline{R}_{y,ac,R}(\tau) = \frac{1}{MT_s} \int_0^{MT_s} E[y_{ac,R}(t)y_{ac,R}(t-\tau)]dt.$$

$$\overline{R}_{y,ac,I}(\tau) = \frac{1}{MT_s} \int_0^{MT_s} E[y_{ac,I}(t)y_{ac,I}(t-\tau)]dt.$$

Proof: Since the analog clipper in Fig. 5.3 can be also modeled by the two identical and individual clipping function $g(\cdot)$, which are the same as digital clipper, and $f(y_{R,t}, y_{R,t-\tau}, y_{I,t}, y_{I,t-\tau}) = f(y_{R,t}, y_{R,t-\tau}) \cdot f(y_{I,t}, y_{I,t-\tau})$ has been given in Lemma 12, therefore, the first conclusion can directly made from Lemma 6. Next, since

$$E[y_{ac}(t)y_{ac}^*(t-\tau)] = E[y_{ac,R}(t)y_{ac,R}(t-\tau)] + E[y_{ac,I}(t)y_{ac,I}(t-\tau)], \quad (5.11)$$

integration on both side still remains the same, that is,

$$\begin{aligned} \frac{1}{MT_s} \int_0^{MT_s} E[y_{ac}(t)y_{ac}^*(t-\tau)]dt &= \frac{1}{MT_s} \int_0^{MT_s} E[y_{ac,R}(t)y_{ac,R}(t-\tau)]dt \\ &+ \frac{1}{MT_s} \int_0^{MT_s} E[y_{ac,I}(t)y_{ac,I}(t-\tau)]dt, \end{aligned} \quad (5.12)$$

Hence, according to the definition, we have

$$\overline{R}_{y,ac}(\tau) = \overline{R}_{y,ac,R}(\tau) + \overline{R}_{y,ac,I}(\tau). \quad (5.13)$$

△△△

Now we put the focus on deriving the average autocorrelation of $y_{ac}(t)$ in Fig. 5.3, that is, derivation of $\overline{R}_{y,ac}(\tau)$.

Lemma 16 : If the analog clipper input signal $y(t)$ is WSCS, then $\overline{R}_{y,ac}(\tau)$, the average autocorrelation of clipper output signal $y_{ac}(t)$, can be expressed as

$$\begin{aligned} \overline{R}_{y,ac}(\tau) &= \frac{2}{MT_s} \int_0^{MT_s} \operatorname{erf}\left(\frac{A}{\sqrt{2}\sigma_{y_{R,t}}}\right) \operatorname{erf}\left(\frac{A}{\sqrt{2}\sigma_{y_{R,t-\tau}}}\right) E[y_{R,t}y_{R,t-\tau}^*] dt \\ &\quad + \frac{2}{MT_s} \int_0^{MT_s} \sum_{m=2,4,\dots}^{\infty} D_m E^{m+1}[y_{R,t}y_{R,t-\tau}] dt \end{aligned}$$

where

$$D_m = \frac{4H_{m-1}\left(\frac{A}{\sqrt{2}\sigma_{y_{R,t}}}\right)H_{m-1}\left(\frac{A}{\sqrt{2}\sigma_{y_{R,t-\tau}}}\right)}{\pi \cdot 2^m \cdot (m+1)! \cdot \sigma_{y_{R,t}}^m \cdot \sigma_{y_{R,t-\tau}}^m} \exp\left(-\frac{A^2}{2\sigma_{y_{R,t}}^2}\right) \exp\left(-\frac{A^2}{2\sigma_{y_{R,t-\tau}}^2}\right).$$

Proof: The explicit derivation will be given in Appendix H. △△△



Chapter 6

Numerical Simulation

6.1 Spectrums of Analog Representation and DFT-Based Implementation of OFDM Transmitters

Notice that we mentioned before that analog representation and commonly used DFT-Based implementation OFDM transmitter differs in spectral roll-off [17], and hence it is improper to use the analog representation modeling to analyze the clipping noise. To see how much the difference is, we then display both the spectrum of $x(t)$ and $y(t)$ in Fig. 1.1 and Fig. 1.2.

Consider the DFT size $M = 64$. The OFDM input signal x_k is a white, Gaussian distributed random process with zero mean and variance σ_x^2 . In the analog representation of the OFDM transmitter, $p(t)$ is a rectangular pulse given by

$$p(t) = \begin{cases} 1, & 0 \leq t < T_0 \\ 0, & o.w. \end{cases} \quad (6.1)$$

where $T_0 = 2\pi/\Omega_0$. The frequency response of $p(t)$ is shown in Fig. 6.1.

As to the commonly used DFT-Based implementation, the window $w(n)$ in OFDM system realization is a discrete rectangular window with coefficients

$$w(n) = \begin{cases} 1, & 0 \leq n \leq M - 1 \\ 0, & othewise \end{cases} \quad (6.2)$$

The reconstruction filter $h(t)$ of the DAC is chosen to be a zero-order hold followed by a second-order elliptical filter [22], that is, $h(t) = h_{ZOH}(t) * h_{ellip}(t)$, where the

zero-order hold $h_{ZOH}(t)$ can be expressed as

$$h_{ZOH}(t) = \begin{cases} 1, & 0 \leq t < T_s \\ 0, & o.w. \end{cases}, \quad (6.3)$$

where T_s is the sampling period, and the parameters of the elliptical filter $h_{ellip}(t)$ as follows: Passband ripple size = 1 dB, stopband attenuation = 20 dB, and natural frequency = $0.5\Omega_s$, where $\Omega_s = 2\pi/T_s$. We plot the frequency response of the reconstruction filter $h(t)$ in Fig. 6.2.

Now we are able to compare the average power spectrum of the output of these two transmitters in Fig. 6.3. The maximum value of these two spectrums has been normalized to one and we can see that the spectral roll-off are quite different. Hence, analog representation modeling is not suitable for analyzing the out-of-band noise for its spectral roll-off is way imprecise from the commonly used model.

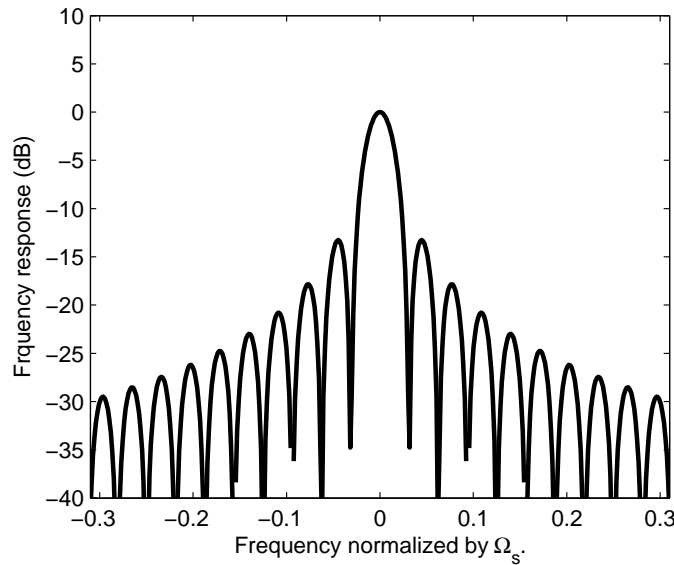


Figure 6.1: Frequency response of the pulse shaping filter $p(t)$ in Fig. 1.1.

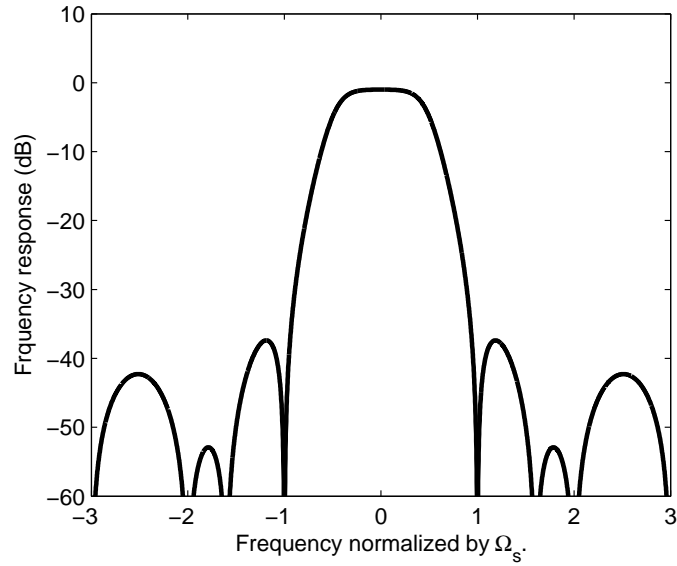


Figure 6.2: Frequency response of reconstruction filter $h(t)$ in Fig. 1.2.

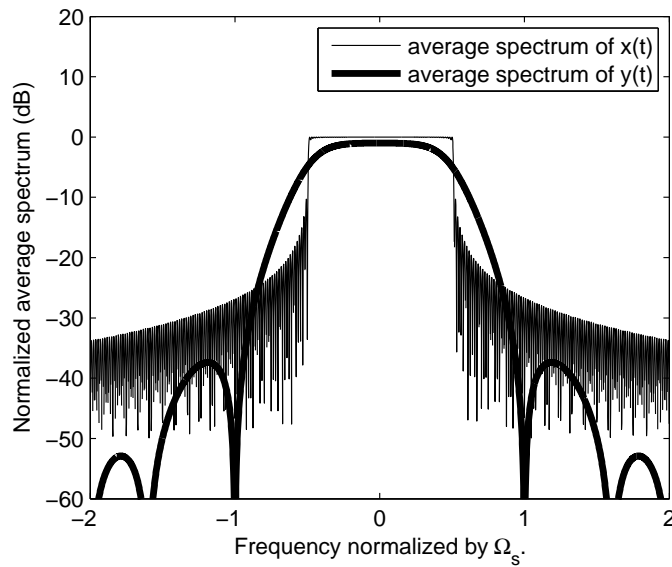


Figure 6.3: Average power spectral densities of the output of the two modulation models $x(t)$ and $y(t)$.

6.2 Digital Clipping in OFDM system

We will use results derived in earlier chapters to plot the average power spectrum of proposed conclusion on the digital clipped OFDM signal.

We will use the models of the OFDM transmitter with digital and analog clipper in Fig. 4.1. The parameters of $w(n)$ and $h(t)$ are the same as the previous section. According to the block diagram in Fig. 4.2, we know that a digital clipper can be modeled by two identical and separate clipping functions $g(\cdot)$ that clips the real and imaginary part of the clipper input signal individually. The clipping function $g(\cdot)$ is as defined in (4.1).

Firstly, consider the parameters $M = 64$, the clipping ratio $A/\sigma_{y_{R,n}}$ can be reduced to A/σ_x from (G.37), which is independent of the variable n . Hence, the notation n can be dropped. The spectrum of $y_{dc}(n)$, which is the digital clipper output in Fig. 4.1, is shown in Fig. 6.4. The clipping ratio $A/\sigma_{y_R} = 1$. Notice that $y_{dc}(n)$ is the digitally clipped signal of $y(n)$. From Lemma 5, we know that the average autocorrelation of $y(n)$ stated in (D.11) is

$$\overline{R}_y(k) = \frac{1}{M} \sum_{n=0}^{M-1} \sigma_x^2 w(n)w(n-k)\delta(k), \quad (6.4)$$

since $w(n)$ is a rectangular window, $\overline{R}_y(k)$ becomes $\sigma_x^2\delta(k)$ and its spectrum $\overline{S}_y(e^{j\omega})$ is white. Hence, from (G.36), we know that $\overline{S}_{y,dc}(e^{j\omega})$, the average spectrum the digital clipper output $y_{dc}(n)$, is also white with only scaling difference from $\overline{S}_y(e^{j\omega})$.

Next, The average spectrum of $y_{dc}(t)$ is considered. Since $\overline{R}_{y,dc}(k)$ is a single pulse, $\overline{R}_{y,dc}(\tau)$ in (B.10) becomes

$$\begin{aligned} \overline{R}_{y,dc}(\tau) &= \frac{C}{T_s} f(\tau) \\ &= \frac{C}{T_s} h(\tau) * h(-\tau) \end{aligned} \quad (6.5)$$

where C is a known constant from the combination of Hermite polynomials and $h(\tau)$ is the reconstruction filter in Fig. 4.1. $\overline{S}_{y,dc}(j\Omega)$ then becomes

$$\overline{S}_{y,dc}(j\Omega) = \frac{C}{T_s} |H(j\Omega)|^2, \quad (6.6)$$

where $H(j\Omega)$ is the frequency response of the reconstruction filter $h(t)$. The figures given in Fig. 6.5 -6.8 are the figures for clipping ratio 0.1, 0.5, 1, 3, respectively. The spectrum of In-band Signal is the first term in (G.36) which relates to the spectrum of clipper input signal. The spectrums of D_2 , D_4 and D_6 are the second term in (G.36) with $m = 2$, $m = 4$ and $m = 6$, which consists in clipping noise. We can see that as the clipping ratio increases, the in-band signal is enlarged and the clipping noise is suppressed.

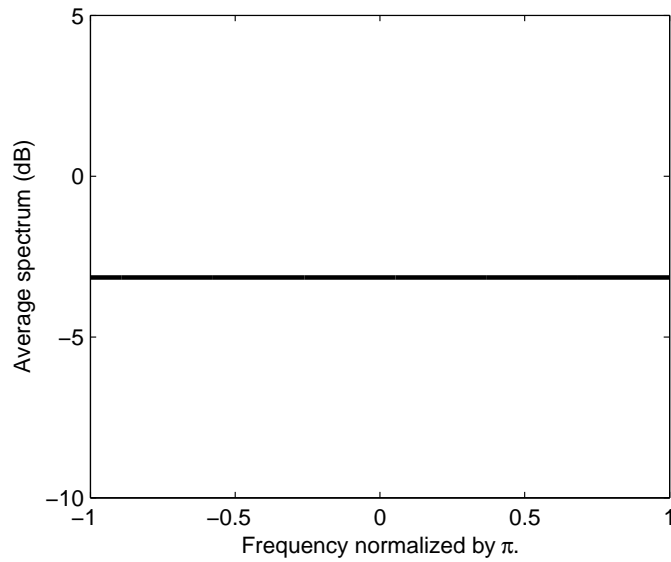


Figure 6.4: Average power spectrum of the digital clipper output $\bar{S}_{y,dc}(e^{j\omega})$.

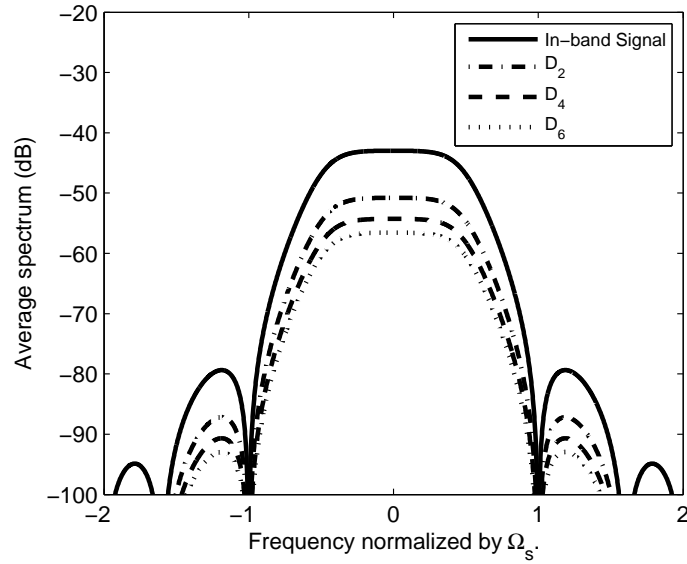


Figure 6.5: Average power spectrum of the OFDM transmitter with digital clipper $\bar{S}_{y,dc}(e^{j\Omega})$. The clipping ratio $A/\sigma_{y_R} = 0.1$.

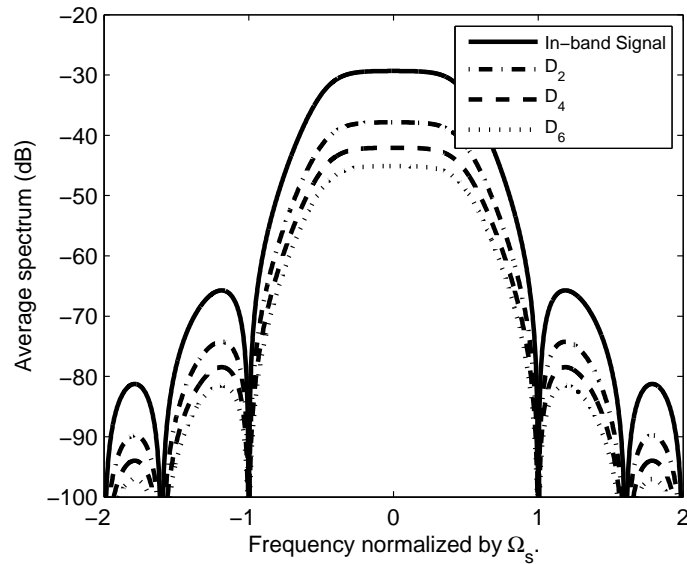


Figure 6.6: Average power spectrum of the OFDM transmitter with digital clipper $\bar{S}_{y,dc}(e^{j\Omega})$. The clipping ratio $A/\sigma_{y_R} = 0.5$.

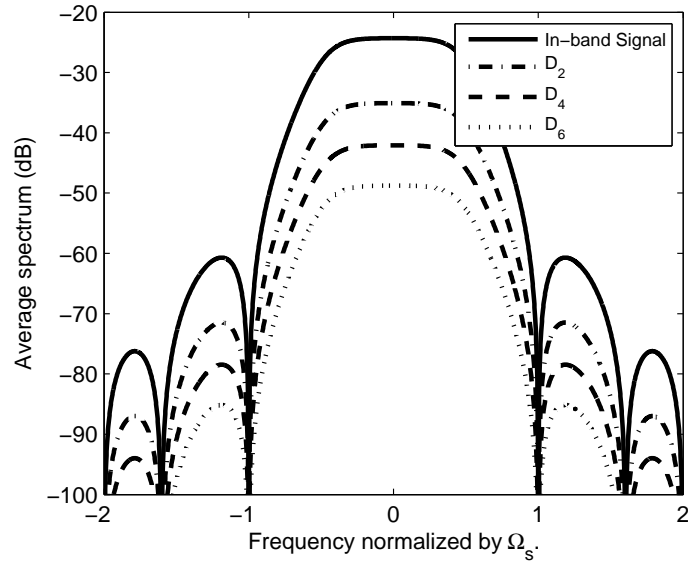


Figure 6.7: Average power spectrum of the OFDM transmitter with digital clipper $\bar{S}_{y,dc}(e^{j\Omega})$. The clipping ratio $A/\sigma_{y_R} = 1$.

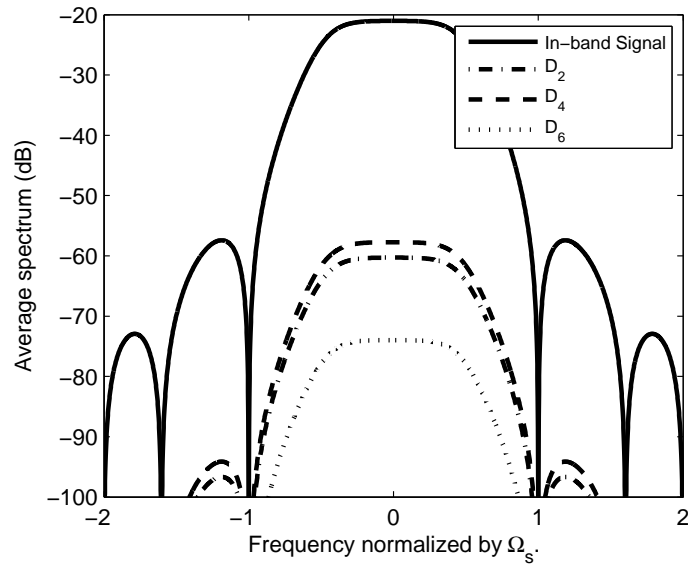


Figure 6.8: Average power spectrum of the OFDM transmitter with digital clipper $\bar{S}_{y,dc}(e^{j\Omega})$. The clipping ratio $A/\sigma_{y_R} = 3$.

6.3 Analog Clipping in OFDM system

We will plot the average power spectrum of proposed conclusion on the analog clipped OFDM signal.

We will use the models of the OFDM transmitter with digital and analog clipper in Fig. 5.1. The parameters of $w(n)$ and $h(t)$ are the same as the previous section. According to the block diagram in Fig. 5.3, we know that an analog clipper can also be modeled by two identical and separate clipping functions $g(\cdot)$ that clips the real and imaginary part of the clipper input signal individually.

As to $\bar{R}_{y,dc}(\tau)$ in (H.36), since $E^{m+1}[y_{R,t}y_{R,t-\tau}]$ convolves itself for $m + 1$ times in frequency domain, it is predictable that the spectrum of the OFDM transmitter with the analog clipper output $y_{ac}(t)$ will spread much more broadly than that $y_{dc}(t)$. However, (H.36) is not a closed form solution, hence, numerical computation is used to resolve the equation. Consider the case DFT size $M = 64$. The clipping ratio $A/\sigma_{y_{R,t}}$ here is a function of time t , therefore, we take the time average on $\sigma_{y_{R,t}}$, where the average clipping ratio is defined as

$$A/\bar{\sigma}_{y_R} \triangleq \frac{A}{\sqrt{\langle \sigma_{y_{R,t}} \rangle}} = \frac{A}{\sqrt{\lim_{\beta \rightarrow \infty} \frac{1}{\beta} \int_{-\beta/2}^{\beta/2} \sigma_{y_{R,t}}^2 dt}} \quad (6.7)$$

The figures given in Fig. 6.9 - 6.12 are the figure for clipping ratio 0.1, 0.5, 1, 3, respectively. The spectrum of In-band Signal is the first term in (H.36) which relates to the spectrum of clipper input signal. The spectrums of D_2 , D_4 and D_6 are the second term in (H.36) with $m = 2$, $m = 4$ and $m = 6$, which consists in clipping noise. A similar result to the digital clipping, as the clipping ratio increases, the in-band signal is enlarged and the clipping noise is suppressed.

Before the end of this section, the comparisons between the OFDM transmitter with two clippers are also shown in Fig. 6.13-6.15. The clipping ratio for the figure are 1, 3, 10. We can see that the spectrum of the system with the analog clipper indeed spreads more broadly than the one with the digital clipper. Furthermore, the increasing the value of clipping ratio, the more similar the two spectrums. The reason why they become so similar due to that larger clipping ratio means clipping free, therefore, the OFDM transmitter with two clippers in Fig. 4.1 and

Fig. 5.1 are simply reduced to the model in Fig. 1.2.

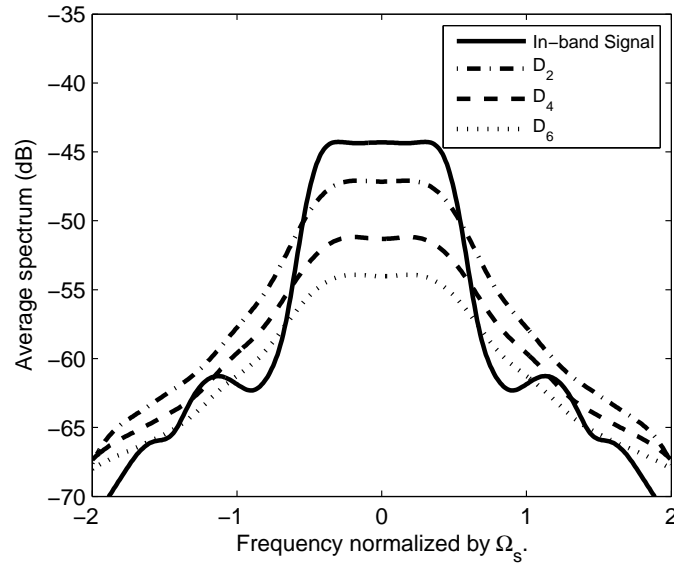


Figure 6.9: Average power spectrum of the OFDM transmitter with analog clipper $\bar{S}_{y,ac}(j\Omega)$. The clipping ratio $A/\bar{\sigma}_{yR} = 0.1$.



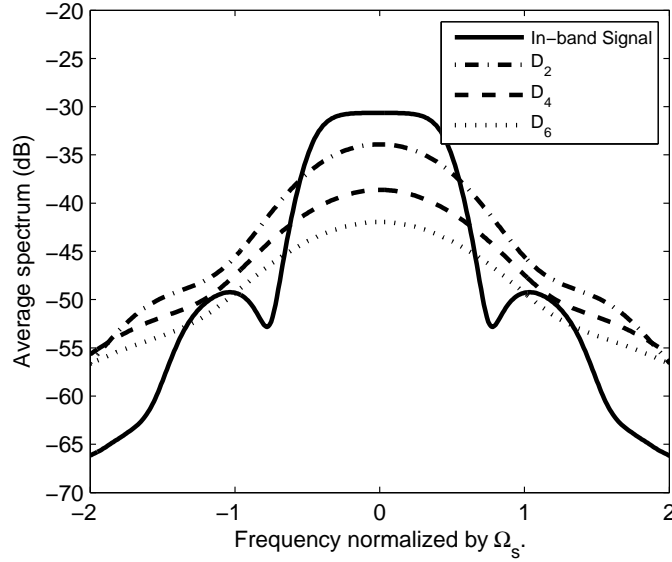


Figure 6.10: Average power spectrum of the OFDM transmitter with analog clipper $\bar{S}_{y,ac}(j\Omega)$. The clipping ratio $A/\bar{\sigma}_{yR} = 0.5$.

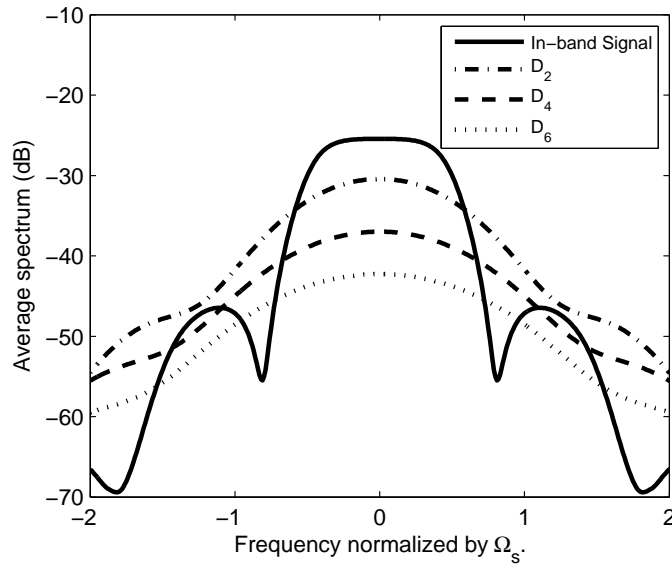


Figure 6.11: Average power spectrum of the OFDM transmitter with analog clipper $\bar{S}_{y,ac}(j\Omega)$. The clipping ratio $A/\bar{\sigma}_{yR} = 1$.

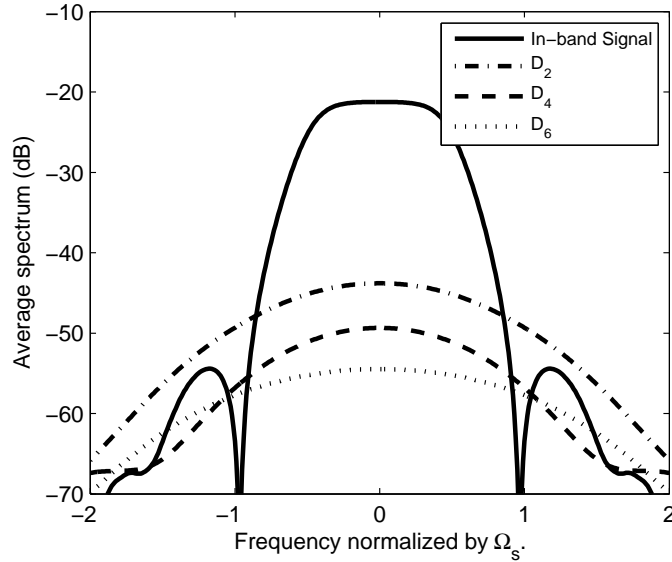


Figure 6.12: Average power spectrum of the OFDM transmitter with analog clipper $\bar{S}_{y,ac}(j\Omega)$. The clipping ratio $A/\bar{\sigma}_{y_R} = 3$.

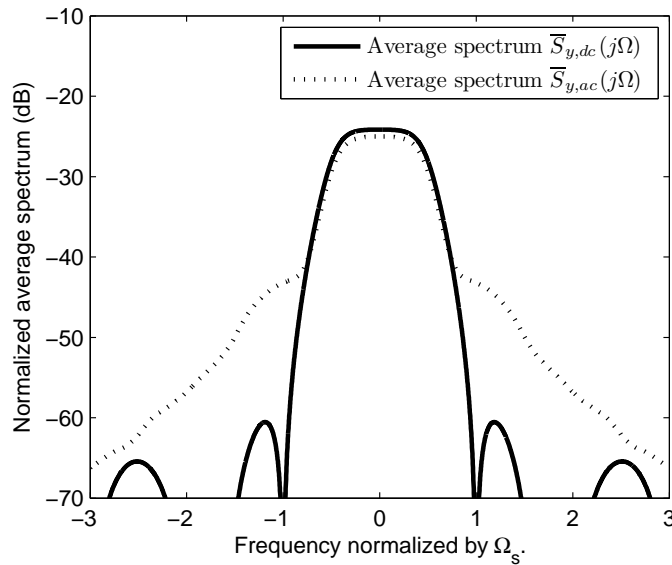


Figure 6.13: Average power spectrum of the two OFDM transmitters with digital and analog clipper, $\bar{S}_{y,dc}(j\Omega)$ and $\bar{S}_{y,ac}(j\Omega)$, respectively. The clipping ratio $A/\sigma_{y_R} = A/\bar{\sigma}_{y_R} = 1$.

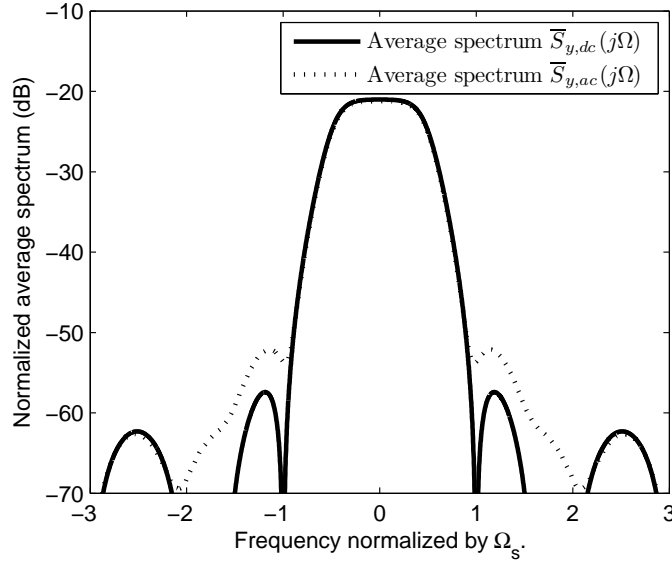


Figure 6.14: Average power spectrum of the two OFDM transmitters with digital and analog clipper, $\bar{S}_{y,dc}(j\Omega)$ and $\bar{S}_{y,ac}(j\Omega)$, respectively. The clipping ratio $A/\sigma_{y_R} = A/\bar{\sigma}_{y_R} = 3$.

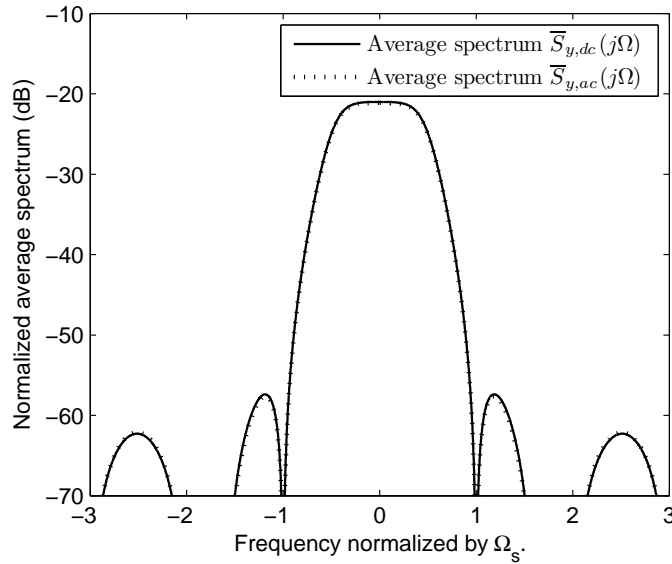


Figure 6.15: Average power spectrum of the two OFDM transmitters with digital and analog clipper, $\bar{S}_{y,dc}(j\Omega)$ and $\bar{S}_{y,ac}(j\Omega)$, respectively. The clipping ratio $A/\sigma_{y_R} = A/\bar{\sigma}_{y_R} = 10$.

6.4 Different Assumption for the Clipper Input Signal

We mentioned that the inappropriate assumption of the clipper input signal also results in a imprecise analysis. In earlier investigations [11, 16], the clipper input signal is assumed to be WSS. According to Lemma 13, the clipper input signal $y(t)$ in Fig. 5.1 is not a WSS process but a WSCS process. If we assume the clipper input signal $y(t)$ in Fig. 5.1 is WSS, then the parameters $\sigma_{y_{R,t}}$ and $\sigma_{y_{R,t-\tau}}$ in (H.36) becomes a constant and

$$\frac{1}{MT_s} \int_0^{MT_s} E[y_{R,t}y_{R,t-\tau}]dt = E[y_{R,t}y_{R,t-\tau}] = h(\tau) * h(-\tau). \quad (6.8)$$

We denote $\sigma_{y_{R,t}} = \sigma_{y_{R,t-\tau}} = \sigma$. This inadequate assumption will underestimate the out-of-band noise. This effect is shown in Fig. 6.16- 6.19. We can observe that the out-of-band noise for WSCS case is greater than the WSS case, hence, one wish to mitigate the clipping noise especially on suppressing the out-of-band noise should not use the WSS assumption for design.

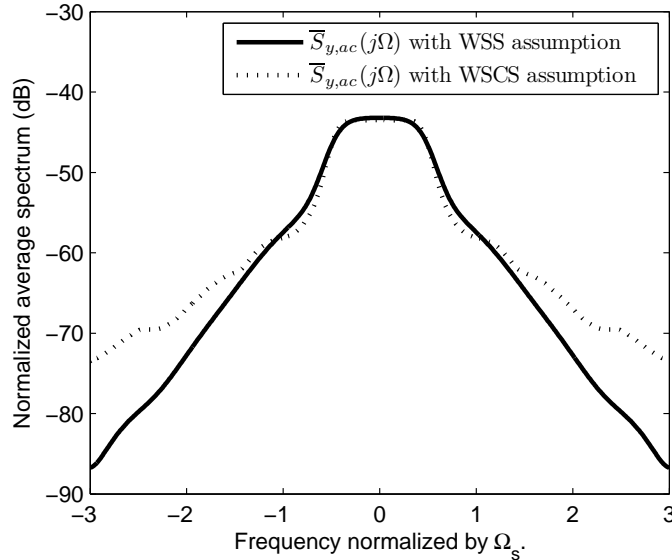


Figure 6.16: $\bar{S}_{y,ac}(j\Omega)$ with the clipper input under the WSS and WSCS assumption. The clipping ratio $A/\sigma = A/\bar{\sigma}_{y_R} = 0.1$.

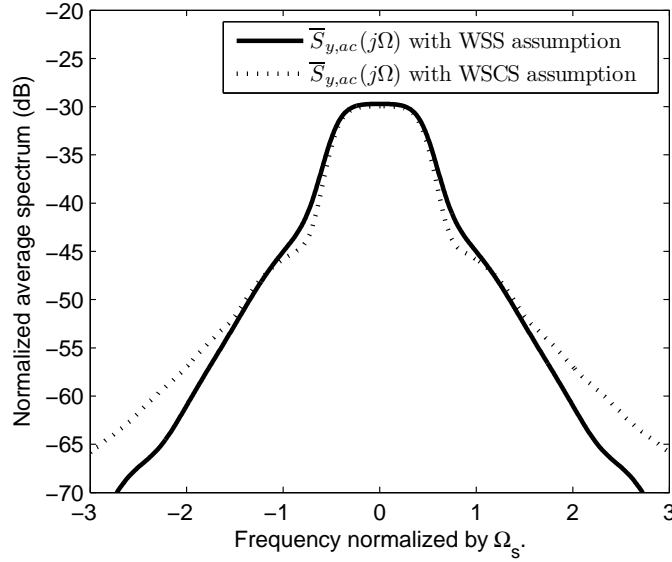


Figure 6.17: $\bar{S}_{y,ac}(j\Omega)$ with the clipper input under the WSS and WSCS assumption. The clipping ratio $A/\sigma = A/\bar{\sigma}_{y_R} = 0.5$.

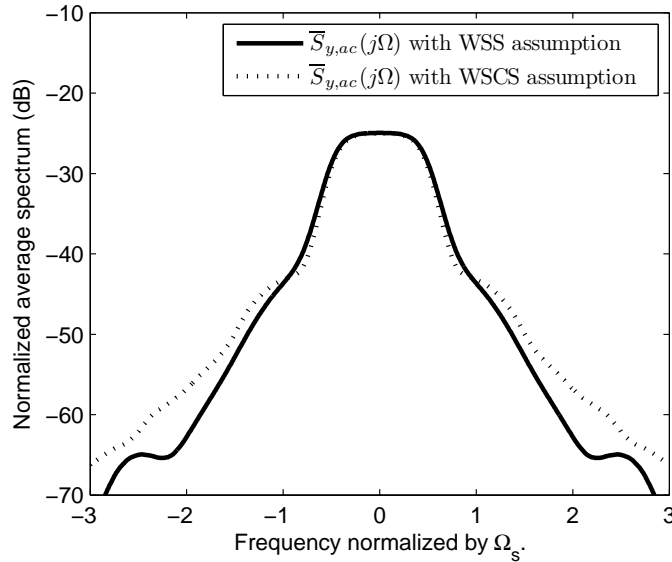


Figure 6.18: $\bar{S}_{y,ac}(j\Omega)$ with the clipper input under the WSS and WSCS assumption. The clipping ratio $A/\sigma = A/\bar{\sigma}_{y_R} = 1$.

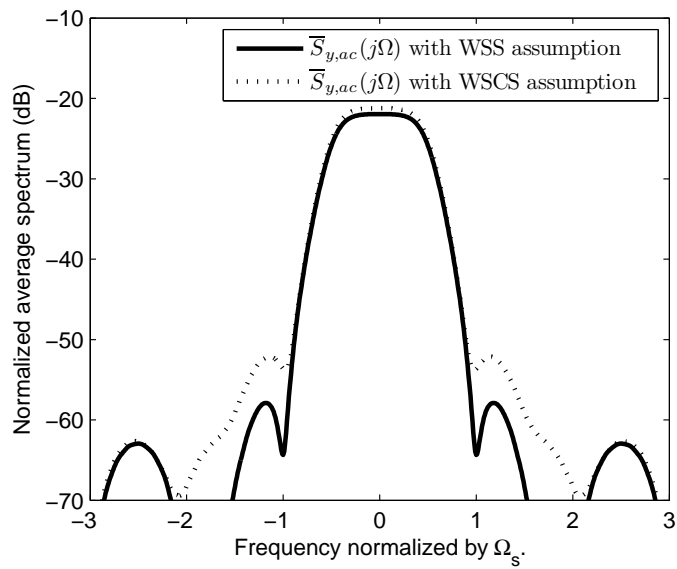


Figure 6.19: $\bar{S}_{y,ac}(j\Omega)$ with the clipper input under the WSS and WSCS assumption. The clipping ratio $A/\sigma = A/\bar{\sigma}_{y_R} = 3$.

Chapter 7

Conclusion

In this thesis, we proposed the analysis of digital and analog clipping in OFDM system. The proposed analysis derives the autocorrelation of the two transmitters under the assumption the clipper input signal is WSCS. Simulation shows the difference of spectral roll-off between the modulators that are of analog representation and DFT-Based implementation. The spectrums of the OFDM transmitter with the digital and analog clipping are shown. The comparison shows that the OFDM transmitter with the analog clipper spreads more widely than digital clipper one in the spectrum. It is shown that digital clipping is a preferred choice especially when clipping ratio is small. The simulation also demonstrates that the assumption that the input signal of the clipper is WSS is inadequate and the clipping noise will be underestimated.

Appendix A

Proof of Lemma 1

From the block diagram in Fig. 2.2, we know that

$$x(t) = \sum_{n=-\infty}^{\infty} x(n)p_1(t - nT). \quad (\text{A.1})$$

Hence, the mean of $x(t)$ and $x(t + MT)$ are

$$E[x(t)] = \sum_{n=-\infty}^{\infty} E[x(n)]p_1(t - nT), \quad (\text{A.2})$$

$$\begin{aligned} E[x(t + MT)] &= \sum_{n=-\infty}^{\infty} E[x(n)]p_1(t + MT - nT) \\ &= \sum_{n=-\infty}^{\infty} E[x(n + M)]p_1(t - nT). \end{aligned} \quad (\text{A.3})$$

Since $x(n)$ is a WSCS(M) process, we have

$$E[x(n)] = E[x(n + M)]. \quad (\text{A.4})$$

Therefore, (A.2) and (A.3) are the same, that is, their means are the same. We then check the autocorrelation of $x(t)$ and $x(t + MT)$

$$E[x(t)x^*(t - \tau)] = \sum_{n=-\infty}^{\infty} \sum_{m=-\infty}^{\infty} E[x(n)x^*(m)]p_1(t - nT)p_1(t - \tau - mT) \quad (\text{A.5})$$

$$\begin{aligned}
E[x(t + MT)x^*(t - \tau + MT)] &= \sum_{n=-\infty}^{\infty} \sum_{m=-\infty}^{\infty} E[x(n)x^*(m)] \cdot \\
&\quad p_1(t - nT + MT)p_1(t - \tau - mT + MT) \\
&= \sum_{n=-\infty}^{\infty} \sum_{m=-\infty}^{\infty} E[x(n + M)x^*(m + M)] \cdot \\
&\quad p_1(t - nT)p_1(t - \tau - mT)
\end{aligned} \tag{A.6}$$

For $x(n)$ is WSCS(M), we also have

$$E[x(n)x^*(m)] = E[x(n + M)x^*(m + M)]. \tag{A.7}$$

Hence, we also know that (A.5) and (A.6) are the same. From above two conclusion, we know that $x(t)$ is a WSCS process with period MT .



Appendix B

Proof of Lemma 2

$$\bar{R}_x(\tau) = \frac{1}{MT} \int_0^{MT} E[x(t)x^*(t-\tau)]dt. \quad (\text{B.1})$$

According to (A.5), we have

$$\bar{R}_x(\tau) = \frac{1}{MT} \sum_{n=-\infty}^{\infty} \sum_{m=-\infty}^{\infty} E[x(n)x^*(m)] \int_0^{MT} p_1(t-nT)p_1(t-\tau-mT)dt. \quad (\text{B.2})$$

Let $m = n - k$, (B.2) becomes

$$\bar{R}_x(\tau) = \frac{1}{T} \sum_{k=-\infty}^{\infty} \frac{1}{M} \left(\sum_{n=-\infty}^{\infty} E[x(n)x^*(n-k)] \cdot \int_0^{MT} p_1(t-nT)p_1(t-\tau-nT+kT)dt \right). \quad (\text{B.3})$$

Gathering M terms of index n in a group, we have

$$\begin{aligned}
\bar{R}_x(\tau) &= \frac{1}{T} \sum_{k=-\infty}^{\infty} \frac{1}{M} \left(\cdots \right. \\
&+ \sum_{n=-M}^{-1} E[x(n)x^*(n-k)] \int_0^{MT} p_1(t-nT)p_1(t-\tau-nT+kT)dt \\
&+ \sum_{n=0}^{M-1} E[x(n)x^*(n-k)] \int_0^{MT} p_1(t-nT)p_1(t-\tau-nT+kT)dt \\
&+ \sum_{n=M}^{2M-1} E[x(n)x^*(n-k)] \int_0^{MT} p_1(t-nT)p_1(t-\tau-nT+kT)dt \\
&\left. + \cdots \right)
\end{aligned} \tag{B.4}$$

The index of n can be changed as

$$\begin{aligned}
\bar{R}_x(\tau) &= \frac{1}{T} \sum_{k=-\infty}^{\infty} \frac{1}{M} \left(\cdots \right. \\
&+ \sum_{n=0}^{M-1} E[x(n-M)x^*(n-k-M)] \cdot \\
&\quad \int_0^{MT} p_1(t-nT+MT)p_1(t-\tau-nT+kT+MTs)dt \\
&+ \sum_{n=0}^{M-1} E[x(n)x^*(n-k)] \int_0^{MT} p_1(t-nT)p_1(t-\tau-nT+kT)dt \\
&+ \sum_{n=0}^{M-1} E[x(n+M)x^*(n-k+M)] \cdot \\
&\quad \int_0^{MT} p_1(t-nT-MT)p_1(t-\tau-nT+kT-MT)dt \\
&\left. + \cdots \right),
\end{aligned} \tag{B.5}$$

we know that $x(n)$ is a WSCS(M) process, therefore,

$$E[x(n)x^*(n-k)] = E[x(n+\gamma M)x^*(n-k+\gamma M)], \quad \forall \gamma \in \mathbb{Z}. \tag{B.6}$$

Then (B.5) is reduced as

$$\begin{aligned}
\bar{R}_x(\tau) = & \frac{1}{T} \sum_{k=-\infty}^{\infty} \frac{1}{M} \left(\cdots \right. \\
& + \sum_{n=0}^{M-1} E[x(n)x^*(n-k)] \cdot \\
& \int_0^{MT} p_1(t-nT+MT)p_1(t-\tau-nT+kT+MTs)dt \\
& + \sum_{n=0}^{M-1} E[x(n)x^*(n-k)] \int_0^{MT} p_1(t-nT)p_1(t-\tau-nT+kT)dt \\
& + \sum_{n=0}^{M-1} E[x(n)x^*(n-k)] \cdot \\
& \int_0^{MT} p_1(t-nT-MT)p_1(t-\tau-nT+kT-MT)dt \\
& \left. + \cdots \right). \tag{B.7}
\end{aligned}$$

Moreover, the intervals of the integrals can also be changed, then (B.7) becomes

$$\begin{aligned}
\bar{R}_x(\tau) = & \frac{1}{T} \sum_{k=-\infty}^{\infty} \frac{1}{M} \left(\cdots \right. \\
& + \sum_{n=0}^{M-1} E[x(n)x^*(n-k)] \int_{MT}^{2MT} p_1(t-nT)p_1(t-\tau-nT+kT)dt \\
& + \sum_{n=0}^{M-1} E[x(n)x^*(n-k)] \int_0^{MT} p_1(t-nT)p_1(t-\tau-nT+kT)dt \\
& + \sum_{n=0}^{M-1} E[x(n)x^*(n-k)] \int_{-MT}^0 p_1(t-nT)p_1(t-\tau-nT+kT)dt \\
& \left. + \cdots \right), \tag{B.8}
\end{aligned}$$

We collect all the other intervals of the integrals, (B.8) results in

$$\begin{aligned}
\bar{R}_x(\tau) &= \frac{1}{T} \sum_{k=-\infty}^{\infty} \frac{1}{M} \sum_{n=0}^{M-1} E[x(n)x^*(n-k)] \left(\cdots \right. \\
&\quad + \int_{MT}^{2MT} p_1(t-nT)p_1(t-\tau-nT+kT)dt \\
&\quad + \int_0^{MT} p_1(t-nT)p_1(t-\tau-nT+kT)dt \\
&\quad \left. + \int_{-MT}^0 p_1(t-nT)p_1(t-\tau-nT+kT)dt + \cdots \right),
\end{aligned} \tag{B.9}$$

then the conclusion can derived as

$$\begin{aligned}
\bar{R}_x(\tau) &= \frac{1}{T} \sum_{k=-\infty}^{\infty} \left(\frac{1}{M} \sum_{n=0}^{M-1} E[x(n)x^*(n-k)] \right) \cdot \left(\int_{-\infty}^{\infty} p_1(t-nT)p_1(t-\tau-nT+kT)dt \right) \\
&= \frac{1}{T} \sum_{k=-\infty}^{\infty} \left(\frac{1}{M} \sum_{n=0}^{M-1} E[x(n)x^*(n-k)] \right) \cdot \left(\int_{-\infty}^{\infty} p_1(t)p_1(t-\tau+kT)dt \right) \\
&= \frac{1}{T} \sum_{k=-\infty}^{\infty} \bar{R}_x(k) \cdot \int_{-\infty}^{\infty} p_1(t)p_1(t-(\tau-kT))dt \\
&= \frac{1}{T} \sum_{k=-\infty}^{\infty} \bar{R}_x(k)f(\tau-kT)
\end{aligned} \tag{B.10}$$

Appendix C

Proof of Lemma 3

At the beginning, we wish to show that $E[y(n)] = E[y(n + m)]$.

$$\begin{aligned}
 E[y(n)] &= w(n) \cdot \frac{1}{\sqrt{M}} \sum_{k=-\frac{M}{2}}^{\frac{M}{2}-1} E[x_{k+B(n)M}] e^{j\frac{2\pi}{M}kn} \\
 &= 0 \\
 E[y(n + M)] &= w(n) \cdot \frac{1}{\sqrt{M}} \sum_{k=-\frac{M}{2}}^{\frac{M}{2}-1} E[x_{k+B(n+M)M}] e^{j\frac{2\pi}{M}k(n+M)} \\
 &= 0
 \end{aligned} \tag{C.1}$$

Next, we are going to show that $E[y(n)y^*(m)] = E[y(n + M)y^*(m + M)]$.

$$\begin{aligned}
 E[y(n)y^*(m)] &= E\left[\left(w(n) \cdot \frac{1}{\sqrt{M}} \sum_{k=-\frac{M}{2}}^{\frac{M}{2}-1} x_{k+B(n)M} e^{j\frac{2\pi}{M}kn} \right) \cdot \left(w^*(m) \cdot \frac{1}{\sqrt{M}} \sum_{l=-\frac{M}{2}}^{\frac{M}{2}-1} x_{l+B(m)M}^* e^{-j\frac{2\pi}{M}lm} \right) \right] \\
 &= \frac{1}{M} w(n)w^*(m) \sum_{k=-\frac{M}{2}}^{\frac{M}{2}-1} \sum_{l=-\frac{M}{2}}^{\frac{M}{2}-1} E[x_{k+B(n)M}x_{l+B(m)M}^*] \cdot e^{j\frac{2\pi}{M}(kn-lm)}
 \end{aligned} \tag{C.2}$$

We know that x_k is a white sequence and possesses the property that

$$E[x_l x_m] = \sigma_x^2 \delta(l - m), \tag{C.3}$$

therefore, (C.2) becomes

$$E[y(n)y^*(m)] = \frac{1}{M}\sigma_x^2 w(n)w^*(m) \sum_{k=-\frac{M}{2}}^{\frac{M}{2}-1} \sum_{l=-\frac{M}{2}}^{\frac{M}{2}-1} \delta(k-l+(B(n)-B(m))M) \cdot e^{j\frac{2\pi}{M}(kn-lm)}. \quad (\text{C.4})$$

Now we make an observation on $E[y(n+M)y^*(m+M)]$.

$$\begin{aligned} & E[y(n+M)y^*(m+M)] \\ &= E\left[\left(w(n+M) \cdot \frac{1}{\sqrt{M}} \sum_{k=-\frac{M}{2}}^{\frac{M}{2}-1} x_{k+B(n+M)M} e^{j\frac{2\pi}{M}k(n+M)} \right) \cdot \left(w^*(m+M) \cdot \frac{1}{\sqrt{M}} \sum_{l=-\frac{M}{2}}^{\frac{M}{2}-1} x_{l+B(m+M)M}^* e^{-j\frac{2\pi}{M}l(m+M)} \right) \right] \\ &= \frac{1}{M}\sigma_x^2 w(n+M)w^*(m+M) \sum_{k=-\frac{M}{2}}^{\frac{M}{2}-1} \sum_{l=-\frac{M}{2}}^{\frac{M}{2}-1} \delta(k-l+(B(n+M)-B(m+M))M) \cdot e^{j\frac{2\pi}{M}(k(n+M)-l(m+M))}. \end{aligned} \quad (\text{C.5})$$

Since $B(n) = \lfloor \frac{n}{M} \rfloor$, it is evident that $B(n+M) = B(n) + 1$, hence, (C.5) results in

$$\begin{aligned} & E[y(n+M)y^*(m+M)] \\ &= \frac{1}{M}\sigma_x^2 w(n+M)w^*(m+M) \sum_{k=-\frac{M}{2}}^{\frac{M}{2}-1} \sum_{l=-\frac{M}{2}}^{\frac{M}{2}-1} \delta(k-l+(B(n)+1-(B(m)+1))M) \cdot e^{j\frac{2\pi}{M}(kn-lm+(k-l)M)} \\ &= \frac{1}{M}\sigma_x^2 w(n+M)w^*(m+M) \sum_{k=-\frac{M}{2}}^{\frac{M}{2}-1} \sum_{l=-\frac{M}{2}}^{\frac{M}{2}-1} \delta(k-l+(B(n)-B(m))M) \cdot e^{j\frac{2\pi}{M}(kn-lm)}. \end{aligned} \quad (\text{C.6})$$

Since the same window is used in each block, that is, $w(n) = w(n+M), \forall n$, therefore in (C.4) and (C.6), we have $E[y(n)y^*(m)] = E[y(n+M)y^*(m+M)]$, and from (C.1), we know $E[y(n)] = E[y(n+M)]$, thus the conclusion is made.

Appendix D

Proof of Lemma 5

Define $\alpha(k, n)$ as

$$\alpha(k, n) \triangleq w(n)x_{k+B(n)M} = \alpha_R(k, n) + j\alpha_I(k, n) \quad (\text{D.1})$$

where

$$\alpha_R(k, n) = w(n)a_{k+B(n)M}, \quad \alpha_I(l, m) = w(m)b_{l+B(m)M}. \quad (\text{D.2})$$

Then from (4.3), we can derive that

$$\begin{aligned} E[\alpha_R(k, n)\alpha_I(l, m)] &= w(n)w(m)E[a_{k+B(n)M}b_{l+B(m)M}] \\ &= 0 \end{aligned} \quad (\text{D.3})$$

$$\begin{aligned} E[\alpha_R(k, n)\alpha_R(l, m)] &= E[\alpha_I(k, n)\alpha_I(l, m)] \\ &= \frac{1}{2}\sigma_x^2 w(n)w(m)\delta(k-l+(B(n)-B(m))M). \end{aligned}$$

Now, we focus on $y_R(n)$ and $y_I(n)$,

$$\begin{aligned} y_R(n) &= \frac{1}{\sqrt{M}} \sum_{k=-\frac{M}{2}}^{\frac{M}{2}-1} \alpha_R(k, n) \cos \frac{2\pi}{M} kn - \alpha_I(k, n) \sin \frac{2\pi}{M} kn \\ y_I(m) &= \frac{1}{\sqrt{M}} \sum_{l=-\frac{M}{2}}^{\frac{M}{2}-1} \alpha_R(l, m) \sin \frac{2\pi}{M} lm + \alpha_I(l, m) \cos \frac{2\pi}{M} lm \end{aligned} \quad (\text{D.4})$$

And the cross correlation between $y_R(n)$ and $y_I(m)$ would be

$$\begin{aligned} E[y_R(n)y_I(m)] &= \frac{1}{2M}\sigma_x^2 w(n)w(m) \sum_{k=-\frac{M}{2}}^{\frac{M}{2}-1} \sum_{l=-\frac{M}{2}}^{\frac{M}{2}-1} \delta(k-l+(B(n)-B(m))M) \cdot \\ &\quad (\cos \frac{2\pi}{M} kn \sin \frac{2\pi}{M} lm - \sin \frac{2\pi}{M} kn \cos \frac{2\pi}{M} lm). \end{aligned} \quad (\text{D.5})$$

Since $-M + 1 \leq k - l \leq M - 1$, it is obvious that delta function takes value with only $k = l$ and $B(n) = B(m)$, consequently, (D.5) becomes

$$\begin{aligned}
E[y_R(n)y_I(m)] &= \frac{1}{2M}\sigma_x^2 w(n)w(m) \sum_{k=-\frac{M}{2}}^{\frac{M}{2}-1} \sin \frac{2\pi}{M} k(m-n) \\
&= \frac{1}{2M}\sigma_x^2 w(n)w(m) \sum_{k=0}^{M-1} \sin \frac{2\pi}{M} k(m-n) \\
&= \frac{1}{2M}\sigma_x^2 w(n)w(m) \Im \left\{ \sum_{k=0}^{M-1} e^{j\frac{2\pi}{M} k(m-n)} \right\} \\
&= \frac{1}{2M}\sigma_x^2 w(n)w(m) \Im \left\{ \frac{1-e^{j2\pi(m-n)}}{1-e^{j\frac{2\pi}{M}(m-n)}} \right\}.
\end{aligned} \tag{D.6}$$

Under the condition $B(n) = B(m)$, we have $-M + 1 \leq m - n \leq M - 1$, for this reason, $\Im \left\{ \frac{1-e^{j2\pi(m-n)}}{1-e^{j\frac{2\pi}{M}(m-n)}} \right\} = \Im \{ M\delta(m-n) \} = 0$. Thus, the first conclusion $E[y_R(n)y_I(m)] = 0, \forall n, m \in \mathbb{Z}$ is made.

Secondly, From Lemma 4 and the previous conclusion, we know that $y(n)$ is jointly Gaussian distributed and $E[y_R(n)y_I(m)] = 0, \forall n, m \in \mathbb{Z}$, therefore, the joint pdf $f(y_{R,n}, y_{R,m}, y_{I,n}, y_{I,m})$ evidently turns into

$$f(y_{R,n}, y_{R,m}, y_{I,n}, y_{I,m}) = f(y_{R,n}, y_{R,m}) \cdot f(y_{I,n}, y_{I,m}) \tag{D.7}$$

This is the conclusion of the second statement.

Next, we concentrate on both the autocorrelations of $y_R(n)$ and $y_I(n)$.

$$\begin{aligned}
E[y_R(n)y_R(m)] &= \frac{1}{2M}\sigma_x^2 w(n)w(m) \sum_{k=-\frac{M}{2}}^{\frac{M}{2}-1} \sum_{l=-\frac{M}{2}}^{\frac{M}{2}-1} \delta(k-l + (B(n) - B(m))M) \cdot \\
&\quad (\cos \frac{2\pi}{M} kn \cos \frac{2\pi}{M} lm + \sin \frac{2\pi}{M} kn \sin \frac{2\pi}{M} lm) \\
&= \frac{1}{2M}\sigma_x^2 w(n)w(m) \sum_{k=-\frac{M}{2}}^{\frac{M}{2}-1} \cos \frac{2\pi}{M} k(n-m) \\
&= \frac{1}{2M}\sigma_x^2 w(n)w(m) \Re \{ M\delta[m-n] \} \\
&= \frac{1}{2}\sigma_x^2 w(n)w(m) \delta[m-n]
\end{aligned} \tag{D.8}$$

$$\begin{aligned}
E[y_I(n)y_I(m)] &= \frac{1}{2M}\sigma_x^2 w(n)w(m) \sum_{k=-\frac{M}{2}}^{\frac{M}{2}-1} \sum_{l=-\frac{M}{2}}^{\frac{M}{2}-1} \delta(k-l+(B(n)-B(m))M) \cdot \\
&\quad \left(\sin \frac{2\pi}{M} kn \sin \frac{2\pi}{M} lm + \cos \frac{2\pi}{M} kn \cos \frac{2\pi}{M} lm \right) \\
&= \frac{1}{2}\sigma_x^2 w(n)w(m)\delta[m-n]
\end{aligned} \tag{D.9}$$

The third statement has been proved.

Finally, we can see that $\bar{R}_y(k)$ becomes

$$\begin{aligned}
\bar{R}_y(k) &= \frac{1}{M} \sum_{n=0}^{M-1} E[y(n)y^*(n-k)] \\
&= \frac{1}{M} \sum_{n=0}^{M-1} \left(E[y_R(n)y_R(n-k)] + E[y_I(n)y_I(n-k)] \right. \\
&\quad \left. + E[y_R(n)y_I(n-k)] + E[y_I(n)y_R(n-k)] \right).
\end{aligned} \tag{D.10}$$

From the previous conclusion, we know that

$$E[y_R(n)y_I(n-k)] = E[y_I(n)y_R(n-k)] = 0,$$

hence, we can demonstrate the last statement that

$$\begin{aligned}
\bar{R}_y(k) &= \frac{1}{M} \sum_{n=0}^{M-1} E[y(n)y^*(n-k)] \\
&= \frac{1}{M} \sum_{n=0}^{M-1} \left(E[y_R(n)y_R(n-k)] + E[y_I(n)y_I(n-k)] \right) \\
&= \bar{R}_{y,R}(k) + \bar{R}_{y,I}(k) \\
&= \frac{1}{M} \sum_{n=0}^{M-1} \left(\frac{1}{2}\sigma_x^2 w(n)w(n-k)\delta(k) + \frac{1}{2}\sigma_x^2 w(n)w(n-k)\delta(k) \right) \\
&= \frac{1}{M} \sum_{n=0}^{M-1} \sigma_x^2 w(n)w(n-k)\delta(k)
\end{aligned} \tag{D.11}$$

This completes all the statements stated above.

Appendix E

Proof of Lemma 6

Denote $y_{dc}(n) = y_{dc,n}$, the other similar subscripts are defined in the same manner.

$$\begin{aligned}
 E[y_{dc}(n)y_{dc}^*(n-k)] &= \int_{-\infty}^{\infty} \cdots \int_{-\infty}^{\infty} y_{dc,n} y_{dc,n-k}^* \\
 &\quad f(y_{R,n}, y_{I,n}, y_{R,n-k}, y_{I,n-k}) dy_{R,n} dy_{I,n} dy_{R,n-k} dy_{I,n-k} \\
 &= \int_{-\infty}^{\infty} \cdots \int_{-\infty}^{\infty} \left(y_{dc,R,n} y_{dc,R,n-k} + y_{dc,I,n} y_{dc,I,n-k} \right. \\
 &\quad \left. + j y_{dc,R,n} y_{dc,I,n-k} - j y_{dc,I,n} y_{dc,R,n-k} \right) \\
 &\quad f(y_{R,n}, y_{I,n}, y_{R,n-k}, y_{I,n-k}) dy_{R,n} dy_{I,n} dy_{R,n-k} dy_{I,n-k}
 \end{aligned} \tag{E.1}$$

We make the substitution that $y_{dc,R}(n) = g(y_{R,n})$ and $y_{dc,I}(n) = g(y_{I,n})$, then (E.1) becomes

$$\begin{aligned}
 E[y_{dc}(n)y_{dc}^*(n-k)] &= \int_{-\infty}^{\infty} \cdots \int_{-\infty}^{\infty} \left(g(y_{R,n})g(y_{R,n-k}) + g(y_{I,n})g(y_{I,n-k}) \right. \\
 &\quad \left. + jg(y_{R,n})g(y_{I,n-k}) - jg(y_{I,n})g(y_{R,n-k}) \right) \\
 &\quad f(y_{R,n}, y_{I,n}, y_{R,n-k}, y_{I,n-k}) dy_{R,n} dy_{I,n} dy_{R,n-k} dy_{I,n-k}
 \end{aligned} \tag{E.2}$$

Further simplification can be made to derive the marginal pdf as

$$\begin{aligned}
E[y_{dc}(n)y_{dc}^*(n-k)] &= \int_{-\infty}^{\infty} \int_{-\infty}^{\infty} g(y_{R,n})g(y_{R,n-k})f(y_{R,n}, y_{R,n-k})dy_{R,n}dy_{R,n-k} \\
&\quad + \int_{-\infty}^{\infty} \int_{-\infty}^{\infty} g(y_{I,n})g(y_{I,n-k})f(y_{I,n}, y_{I,n-k})dy_{I,n}dy_{I,n-k} \\
&\quad + j \int_{-\infty}^{\infty} \int_{-\infty}^{\infty} g(y_{R,n})g(y_{I,n-k})f(y_{R,n}, y_{I,n-k})dy_{R,n}dy_{I,n-k} \\
&\quad - j \int_{-\infty}^{\infty} \int_{-\infty}^{\infty} g(y_{I,n})g(y_{R,n-k})f(y_{I,n}, y_{R,n-k})dy_{I,n}dy_{R,n-k}
\end{aligned} \tag{E.3}$$

Now we make an Observation on the first term of the imaginary part in (E.3).

From (D.7), we have

$$f(y_{R,n}, y_{R,n-k}, y_{I,n}, y_{I,n-k}) = f(y_{R,n}, y_{R,n-k}) \cdot f(y_{I,n}, y_{I,n-k}), \tag{E.4}$$

therefore, $f(y_{R,n}, y_{I,n-k})$ in (E.3) becomes

$$f(y_{R,n}, y_{I,n-k}) = f(y_{R,n})f(y_{I,n-k}), \tag{E.5}$$

therefore, the the first term of the imaginary part in (E.3) becomes

$$\begin{aligned}
&j \int_{-\infty}^{\infty} \int_{-\infty}^{\infty} g(y_{R,n})g(y_{I,n-k})f(y_{R,n}, y_{I,n-k})dy_{R,n}dy_{I,n-k} \\
&= j \int_{-\infty}^{\infty} \int_{-\infty}^{\infty} g(y_{R,n})g(y_{I,n-k})f(y_{R,n})f(y_{I,n-k})dy_{R,n}dy_{I,n-k} \\
&= j \int_{-\infty}^{\infty} g(y_{R,n})f(y_{R,n})dy_{R,n} \cdot \int_{-\infty}^{\infty} g(y_{I,n-k})f(y_{I,n-k})dy_{I,n-k} \\
&= j \left(\int_{-\infty}^{-A} (-A)f(y_{R,n})dy_{R,n} + \int_{-A}^A y_{R,n}f(y_{R,n})dy_{R,n} + \int_A^{\infty} Af(y_{R,n})dy_{R,n} \right) \cdot \\
&\quad \int_{-\infty}^{\infty} g(y_{I,n-k})f(y_{I,n-k})dy_{I,n-k}
\end{aligned} \tag{E.6}$$

According to the definition of Q function, we know that (E.6) results in

$$\begin{aligned}
&j \int_{-\infty}^{\infty} \int_{-\infty}^{\infty} g(y_{R,n})g(y_{I,n-k})f(y_{R,n}, y_{I,n-k})dy_{R,n}dy_{I,n-k} \\
&= j \left((-A)Q\left(\frac{A}{\sigma_{y_{R,n}}}\right) + 0 + AQ\left(\frac{A}{\sigma_{y_{R,n}}}\right) \right) \cdot \int_{-\infty}^{\infty} g(y_{I,n-k})f(y_{I,n-k})dy_{I,n-k} \\
&= j \cdot 0 \cdot \int_{-\infty}^{\infty} g(y_{I,n-k})f(y_{I,n-k})dy_{I,n-k} \\
&= 0.
\end{aligned} \tag{E.7}$$

For the similar reason, it is the same that

$$-j \int_{-\infty}^{\infty} \int_{-\infty}^{\infty} g(y_{I,n})g(y_{R,n-k})f(y_{I,n}, y_{R,n-k})dy_{I,n}dy_{R,n-k} = 0. \quad (\text{E.8})$$

Hence,(E.3) becomes

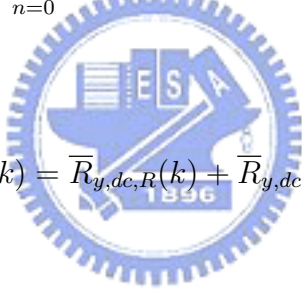
$$\begin{aligned} E[y_{dc}(n)y_{dc}^*(n-k)] &= \int_{-\infty}^{\infty} \cdots \int_{-\infty}^{\infty} g(y_{R,n})g(y_{R,n-k})f(y_{R,n}, y_{R,n-k})dy_{R,n}dy_{R,n-k} \\ &\quad + \int_{-\infty}^{\infty} \cdots \int_{-\infty}^{\infty} g(y_{I,n})g(y_{I,n-k})f(y_{I,n}, y_{I,n-k})dy_{I,n}dy_{I,n-k} \\ &= E[y_{dc,R}(n)y_{dc,R}(n-k)] + E[y_{dc,I}(n)y_{dc,I}(n-k)]. \end{aligned} \quad (\text{E.9})$$

This is the conclusion of the first statement, and from (E.9), it is evident that

$$\sum_{n=0}^{M-1} E[y_{dc}(n)y_{dc}^*(n-k)] = \sum_{n=0}^{M-1} E[y_{dc,R}(n)y_{dc,R}(n-k)] + \sum_{n=0}^{M-1} E[y_{dc,I}(n)y_{dc,I}(n-k)]. \quad (\text{E.10})$$

Thus, by the definition,

$$\bar{R}_{y,dc}(k) = \bar{R}_{y,dc,R}(k) + \bar{R}_{y,dc,I}(k). \quad (\text{E.11})$$



Appendix F

Proof of Lemma 7

We know that $y(n)$ is jointly WSCS with period M and Gaussian distributed. For this reason, the real and imaginary part of $y(n)$, $y_R(n)$ and $y_I(n)$, are also WSCS(M) and Gaussian distributed. As we know, Gaussian distribution only relates to the first and the second moment statistics, and the WSCS property specifies these two statistics that

$$\begin{aligned} E[y(n)] &= E[y(n+M)] \\ E[y(n)y^*(n-k)] &= E[y(n+M)y^*(n-k+M)]. \end{aligned} \tag{F.1}$$

Hence, the joint pdf possesses the following relationship

$$f(y_{R,n}, y_{I,n}, y_{R,n-k}, y_{I,n-k}) = f(y_{R,n+M}, y_{I,n+M}, y_{R,n-k+M}, y_{I,n-k+M}). \tag{F.2}$$

And also, the other joint relationships such as

$$\begin{aligned} f(y_{R,n}) &= f(y_{R,n+M}) \\ f(y_{I,n}) &= f(y_{I,n+M}) \\ f(y_{R,n}, y_{R,n-k}) &= f(y_{R,n+M}, y_{R,n-k+M}) \\ f(y_{I,n}, y_{I,n-k}) &= f(y_{I,n+M}, y_{I,n-k+M}) \end{aligned} \tag{F.3}$$

exist as well. We here wish to prove two properties to show that $y_{dc}(n)$ is WSCS(M), which are

$$\begin{aligned} E[y_{dc}(n)] &= E[y_{dc}(n+M)] \\ E[y_{dc}(n)y_{dc}^*(n-k)] &= E[y_{dc}(n+M)y_{dc}^*(n-k+M)]. \end{aligned} \tag{F.4}$$

Firstly,

$$\begin{aligned}
E[y_{dc}(n)] &= E[y_{dc,R}(n)] + jE[y_{dc,I}(n)] \\
&= \int_{-\infty}^{\infty} g(y_{R,n})f(y_{R,n})dy_{R,n} + j \int_{-\infty}^{\infty} g(y_{I,n})f(y_{I,n})dy_{I,n}
\end{aligned} \tag{F.5}$$

where $g(\cdot)$ is the clipping function.

$$\begin{aligned}
E[y_{dc}(n+M)] &= E[y_{dc,R}(n+M)] + jE[y_{dc,I}(n+M)] \\
&= \int_{-\infty}^{\infty} g(y_{R,n+M})f(y_{R,n+M})dy_{R,n+M} \\
&\quad + j \int_{-\infty}^{\infty} g(y_{I,n+M})f(y_{I,n+M})dy_{I,n+M}
\end{aligned} \tag{F.6}$$

From (F.3), we have

$$f(y_{R,n}) = f(y_{R,n+M}), \quad f(y_{I,n}) = f(y_{I,n+M}) \tag{F.7}$$

Thus, the integrals in (F.5) and (F.6) are exact the same except for dummy variables, which results in $E[y_{dc}(n)] = E[y_{dc}(n+M)]$. Hence we have shown the first part of the statement.

Secondly, it is shown in Lemma 6 that

$$E[y_{dc}(n)y_{dc}^*(n-k)] = E[y_{dc,R}(n)y_{dc,R}(n-k)] + E[y_{dc,I}(n)y_{dc,I}(n-k)], \tag{F.8}$$

therefore, to prove that

$$E[y_{dc}(n)y_{dc}^*(n-k)] = E[y_{dc}(n+M)y_{dc}^*(n-k+M)], \tag{F.9}$$

we only need to show that

$$\begin{aligned}
E[y_{dc,R}(n)y_{dc,R}(n-k)] &= E[y_{dc,R}(n+M)y_{dc,R}(n-k+M)] \\
E[y_{dc,I}(n)y_{dc,I}(n-k)] &= E[y_{dc,I}(n+M)y_{dc,I}(n-k+M)].
\end{aligned} \tag{F.10}$$

The first statement in (F.10) is taken into consideration:

$$E[y_{dc,R}(n)y_{dc,R}(n-k)] = \int_{-\infty}^{\infty} \int_{-\infty}^{\infty} g(y_{R,n})g(y_{R,n-k})f(y_{R,n}, y_{R,n-k})dy_{R,n}dy_{R,n-k} \tag{F.11}$$

$$\begin{aligned}
E[y_{dc,R}(n+M)y_{dc,R}(n-k+M)] &= \int_{-\infty}^{\infty} \int_{-\infty}^{\infty} g(y_{R,n+M})g(y_{R,n-k+M}) \cdot \\
&\quad f(y_{R,n+M}, y_{R,n-k+M}) dy_{R,n+M} dy_{R,n-k+M}
\end{aligned} \tag{F.12}$$

From (F.3), we have

$$f(y_{R,n}, y_{R,n-k}) = f(y_{R,n+M}, y_{R,n-k+M}), \tag{F.13}$$

therefore, in (F.11) and (F.12), the integrals becomes the same, therefore, we have shown that $E[y_{dc,R}(n)y_{dc,R}(n-k)] = E[y_{dc,R}(n+M)y_{dc,R}(n-k+M)]$. The similar deduction can be used to prove $E[y_{dc,I}(n)y_{dc,I}(n-k)] = E[y_{dc,I}(n+M)y_{dc,I}(n-k+M)]$ for that joint relationship

$$f(y_{I,n}, y_{I,n-k}) = f(y_{I,n+M}, y_{I,n-k+M}) \tag{F.14}$$

in (F.3) exists. Eventually, both equations in (F.10) are satisfied. According to the conclusion proved in Lemma 6 in (F.8), we have verified the equation $E[y_{dc}(n)y_{dc}^*(n-k)] = E[y_{dc}(n+M)y_{dc}^*(n-k+M)]$ holds, and thus we finished the second part of the statement.

For these two parts of proofs, we can now claim that the output sequence of the digital clipper $y_{dc}(n)$ is WSCS(M).

Appendix G

Proof of Lemma 8

Base on the conclusion of Lemma 6, we know that

$$\begin{aligned}
 E[y_{dc}(n)y_{dc}^*(n-k)] &= E[y_{dc,R}(n)y_{dc,R}(n-k)] + E[y_{dc,I}(n)y_{dc,I}(n-k)] \\
 &= \int_{-\infty}^{\infty} \int_{-\infty}^{\infty} g(y_{R,n})g(y_{R,n-k})f(y_{R,n}, y_{R,n-k})dy_{R,n}dy_{R,n-k} \\
 &\quad + \int_{-\infty}^{\infty} \int_{-\infty}^{\infty} g(y_{I,n})g(y_{I,n-k})f(y_{I,n}, y_{I,n-k})dy_{I,n}dy_{I,n-k}.
 \end{aligned} \tag{G.1}$$

Since $f(y_{R,n}, y_{R,n-k})$ and $f(y_{I,n}, y_{I,n-k})$ are both Gaussian distributed, and from (D.8) and (D.9), we have the relationship that

$$E[y_{R,n}y_{R,n-k}] = E[y_{I,n}y_{I,n-k}], \tag{G.2}$$

therefore, $f(y_{R,n}, y_{R,n-k}) = f(y_{I,n}, y_{I,n-k})$ and hence the following deduction can only focus on the first integral in (G.1), and the second integral can be derived in the similar manner.

We now emphasize the derivation of $E[y_{dc,R}(n)y_{dc,R}(n-k)]$, that is, to derive the closed form of

$$\int_{-\infty}^{\infty} \int_{-\infty}^{\infty} g(y_{R,n})g(y_{R,n-k})f(y_{R,n}, y_{R,n-k})dy_{R,n}dy_{R,n-k}. \tag{G.3}$$

The joint pdf of $f(y_{R,n}, y_{R,n-k})$ is

$$\begin{aligned}
 f(y_{R,n}, y_{R,n-k}) &= \frac{1}{2\pi\sigma_{y_{R,n}}\sigma_{y_{R,n-k}}\sqrt{1-r^2(n,k)}} \cdot \\
 &\quad \exp\left(-\frac{1}{2(1-r^2(n,k))} \cdot \left(\frac{y_{R,n}^2}{\sigma_{y_{R,n}}^2} - 2r(n,k)\frac{y_{R,n}}{\sigma_{y_{R,n}}}\frac{y_{R,n-k}}{\sigma_{y_{R,n-k}}} + \frac{y_{R,n-k}^2}{\sigma_{y_{R,n-k}}^2}\right)\right)
 \end{aligned} \tag{G.4}$$

where

$$r(n, k) = \frac{E[y_{R,n}y_{R,n-k}]}{\sigma_{y_{R,n}}\sigma_{y_{R,n-k}}} \quad (\text{G.5})$$

By Price's Theorem[18, 20]

$$\begin{aligned} \frac{\partial(E[y_{dc,R,n}y_{dc,R,n-k}])}{\partial(E[y_{R,n}y_{R,n-k}])} &= E\left(\frac{\partial y_{dc,R,n}}{\partial y_{R,n}} \frac{\partial y_{dc,R,n-k}}{\partial y_{R,n-k}}\right) \\ &= E\left(\frac{\partial g(y_{R,n})}{\partial y_{R,n}} \frac{\partial g(y_{R,n-k})}{\partial y_{R,n-k}}\right) \\ &= \int_{-\infty}^{\infty} \int_{-\infty}^{\infty} \frac{\partial g(y_{R,n})}{\partial y_{R,n}} \frac{\partial g(y_{R,n-k})}{\partial y_{R,n-k}} f(y_{R,n}, y_{R,n-k}) dy_{R,n} dy_{R,n-k}. \end{aligned} \quad (\text{G.6})$$

Due to the clipping function $g(\cdot)$, the intervals of the integrals can be divided into several regions, which lies on the linear and the nonlinear intervals of the clipping function. Thus, (G.6) becomes

$$\begin{aligned} \frac{\partial(E[y_{dc,R,n}y_{dc,R,n-k}])}{\partial(E[y_{R,n}y_{R,n-k}])} &= \int_{-A}^A \int_{-A}^A \frac{\partial y_{R,n}}{\partial y_{R,n}} \frac{\partial y_{R,n-k}}{\partial y_{R,n-k}} f(y_{R,n}, y_{R,n-k}) dy_{R,n} dy_{R,n-k} \\ &+ \int_{-A}^A \int_A^{\infty} \frac{\partial A}{\partial y_{R,n}} \frac{\partial y_{R,n-k}}{\partial y_{R,n-k}} f(y_{R,n}, y_{R,n-k}) dy_{R,n} dy_{R,n-k} \\ &+ \int_{-A}^A \int_{-\infty}^{-A} \frac{\partial(-A)}{\partial y_{R,n}} \frac{\partial y_{R,n-k}}{\partial y_{R,n-k}} f(y_{R,n}, y_{R,n-k}) dy_{R,n} dy_{R,n-k} \\ &+ \int_A^{\infty} \int_{-\infty}^{\infty} \frac{\partial g(y_{R,n})}{\partial y_{R,n}} \frac{\partial A}{\partial y_{R,n-k}} f(y_{R,n}, y_{R,n-k}) dy_{R,n} dy_{R,n-k} \\ &+ \int_{-\infty}^{-A} \int_{-\infty}^{\infty} \frac{\partial g(y_{R,n})}{\partial y_{R,n}} \frac{\partial(-A)}{\partial y_{R,n-k}} f(y_{R,n}, y_{R,n-k}) dy_{R,n} dy_{R,n-k}. \end{aligned} \quad (\text{G.7})$$

It is evident that all the integrals are zero except for the first one, therefore, only the first term is left in (G.7), that is,

$$\frac{\partial(E[y_{dc,R,n}y_{dc,R,n-k}])}{\partial(E[y_{R,n}y_{R,n-k}])} = \int_{-A}^A \int_{-A}^A f(y_{R,n}, y_{R,n-k}) dy_{R,n} dy_{R,n-k} \quad (\text{G.8})$$

By Mehler's formula [21], we know that

$$\frac{1}{\sqrt{1-\omega^2}} \exp\left(\frac{-\omega^2\alpha^2+2\omega\alpha\beta-\omega^2\beta^2}{1-\omega^2}\right) = \sum_{m=0}^{\infty} \frac{H_m(\alpha)H_m(\beta)\omega^m}{2^m \cdot m!} \quad (\text{G.9})$$

where $\alpha, \beta, \omega \in \mathbb{R}$ and $H_m(x)$ is the Hermite polynomial and defined as

$$H_m(x) = (-1)^m \exp(x^2) \frac{d^m}{dx^m} \exp(-x^2). \quad (\text{G.10})$$

Therefore, the joint pdf in (G.8) becomes

$$\begin{aligned}
f(y_{R,n}, y_{R,n-k}) &= \frac{1}{2\pi\sigma_{y_{R,n}}\sigma_{y_{R,n-k}}} \cdot \\
&\frac{1}{\sqrt{1-r^2(n,k)}} \exp\left(\frac{-r^2(n,k)\left(\frac{y_{R,n}}{\sqrt{2}\sigma_{y_{R,n}}}\right)^2 + 2r(n,k)\left(\frac{y_{R,n}}{\sqrt{2}\sigma_{y_{R,n}}}\right)\left(\frac{y_{R,n-k}}{\sqrt{2}\sigma_{y_{R,n-k}}}\right) - r^2(n,k)\left(\frac{y_{R,n-k}}{\sqrt{2}\sigma_{y_{R,n-k}}}\right)^2}{1-r^2(n,k)}\right) \cdot \\
&\exp\left(\frac{(r^2(n,k)-1)\left(\frac{y_{R,n}}{\sqrt{2}\sigma_{y_{R,n}}}\right)^2}{1-r^2(n,k)}\right) \cdot \exp\left(\frac{(r^2(n,k)-1)\left(\frac{y_{R,n-k}}{\sqrt{2}\sigma_{y_{R,n-k}}}\right)^2}{1-r^2(n,k)}\right) \\
&= \frac{1}{2\pi\sigma_{y_{R,n}}\sigma_{y_{R,n-k}}} \cdot \sum_{m=0}^{\infty} \frac{H_m\left(\frac{y_{R,n}}{\sqrt{2}\sigma_{y_{R,n}}}\right)H_m\left(\frac{y_{R,n-k}}{\sqrt{2}\sigma_{y_{R,n-k}}}\right)r^m(n,k)}{2^m \cdot m!} \cdot \\
&\exp\left(-\left(\frac{y_{R,n}}{\sqrt{2}\sigma_{y_{R,n}}}\right)^2\right) \cdot \exp\left(-\left(\frac{y_{R,n-k}}{\sqrt{2}\sigma_{y_{R,n-k}}}\right)^2\right), \tag{G.11}
\end{aligned}$$

and (G.8) can be simplified as

$$\begin{aligned}
\frac{\partial(E[y_{dc,R,n}y_{dc,R,n-k}])}{\partial(E[y_{R,n}y_{R,n-k}])} &= \frac{1}{2\pi\sigma_{y_{R,n}}\sigma_{y_{R,n-k}}} \sum_{m=0}^{\infty} \frac{r^m(n,k)}{2^m \cdot m!} \cdot \\
&\int_{-A}^A H_m\left(\frac{y_{R,n}}{\sqrt{2}\sigma_{y_{R,n}}}\right) \exp\left(-\left(\frac{y_{R,n}}{\sqrt{2}\sigma_{y_{R,n}}}\right)^2\right) dy_{R,n} \cdot \\
&\int_{-A}^A H_m\left(\frac{y_{R,n-k}}{\sqrt{2}\sigma_{y_{R,n-k}}}\right) \exp\left(-\left(\frac{y_{R,n-k}}{\sqrt{2}\sigma_{y_{R,n-k}}}\right)^2\right) dy_{R,n-k}. \tag{G.12}
\end{aligned}$$

Let $u = \frac{y_{R,n}}{\sqrt{2}\sigma_{y_{R,n}}}$, the first integral in (G.12) becomes

$$\int_{-A}^A H_m\left(\frac{y_{R,n}}{\sqrt{2}\sigma_{y_{R,n}}}\right) \exp\left(-\left(\frac{y_{R,n}}{\sqrt{2}\sigma_{y_{R,n}}}\right)^2\right) dy_{R,n} = \sqrt{2}\sigma_{y_{R,n}} \int_{-\frac{A}{\sqrt{2}\sigma_{y_{R,n}}}}^{\frac{A}{\sqrt{2}\sigma_{y_{R,n}}}} H_m(u) \exp(-u^2) du, \tag{G.13}$$

then, (G.12) turns into

$$\begin{aligned}
\frac{\partial(E[y_{dc,R,n}y_{dc,R,n-k}])}{\partial(E[y_{R,n}y_{R,n-k}])} &= \frac{1}{\pi} \sum_{m=0}^{\infty} \frac{r^m(n,k)}{2^m \cdot m!} \cdot \int_{-\frac{A}{\sqrt{2}\sigma_{y_{R,n}}}}^{\frac{A}{\sqrt{2}\sigma_{y_{R,n}}}} H_m(u) \exp(-u^2) du \cdot \\
&\int_{-\frac{A}{\sqrt{2}\sigma_{y_{R,n-k}}}}^{\frac{A}{\sqrt{2}\sigma_{y_{R,n-k}}}} H_m(v) \exp(-v^2) dv. \tag{G.14}
\end{aligned}$$

According to the definition of the Hermite polynomial $H_m(x)$ in (G.10), we know that

$$H_m(x) = \begin{cases} \text{even function,} & m \text{ is even} \\ \text{odd function,} & m \text{ is odd} \end{cases}. \quad (\text{G.15})$$

When m is odd, the integrand $H_m(u) \exp(-u^2)$ becomes an odd function. Due to the symmetry of the integral interval,

$$\begin{aligned} \int_{-\frac{\frac{A}{\sqrt{2\sigma_{yR,n}}}}{\frac{A}{\sqrt{2\sigma_{yR,n}}}}^{\frac{A}{\sqrt{2\sigma_{yR,n}}}} H_m(u) \exp(-u^2) du &= 0, \text{ if } m \text{ is odd.} \\ \int_{-\frac{\frac{A}{\sqrt{2\sigma_{yR,n}}}}{\frac{A}{\sqrt{2\sigma_{yR,n}}}}^{\frac{A}{\sqrt{2\sigma_{yR,n}}}} H_m(u) \exp(-u^2) du &= \int_0^{\frac{2A}{\sqrt{2\sigma_{yR,n}}}} H_m(u) \exp(-u^2) du, \text{ if } m \text{ is even.} \end{aligned} \quad (\text{G.16})$$

Similar deduction process can be applied to the second integral in (G.14), then the further simplification of (G.14) can be derived as

$$\begin{aligned} \frac{\partial(E[y_{dc,R,n} y_{dc,R,n-k}])}{\partial(E[y_{R,n} y_{R,n-k}])} &= \frac{1}{\pi} \sum_{m=0,2,4,\dots}^{\infty} \frac{r^m(n,k)}{2^m \cdot m!} \cdot \int_{-\frac{\frac{A}{\sqrt{2\sigma_{yR,n}}}}{\frac{A}{\sqrt{2\sigma_{yR,n}}}}^{\frac{A}{\sqrt{2\sigma_{yR,n}}}} H_m(u) \exp(-u^2) du \cdot \\ &\quad \int_{-\frac{\frac{A}{\sqrt{2\sigma_{yR,n-k}}}}{\frac{A}{\sqrt{2\sigma_{yR,n-k}}}}^{\frac{A}{\sqrt{2\sigma_{yR,n-k}}}} H_m(v) \exp(-v^2) dv. \\ &= \frac{4}{\pi} \sum_{m=0,2,4,\dots}^{\infty} \frac{r^m(n,k)}{2^m \cdot m!} \cdot \int_0^{\frac{A}{\sqrt{2\sigma_{yR,n}}}} H_m(u) \exp(-u^2) du \cdot \\ &\quad \int_0^{\frac{A}{\sqrt{2\sigma_{yR,n-k}}}} H_m(v) \exp(-v^2) dv. \end{aligned} \quad (\text{G.17})$$

We wish to isolate the $m = 0$ term now. Since the error function $erf(x)$ is defined as

$$erf(x) \triangleq \frac{2}{\sqrt{\pi}} \int_0^x \exp(-t^2) dt \quad (\text{G.18})$$

and

$$H_0(x) = 1, \quad \forall x \in \mathbb{R} \quad (\text{G.19})$$

(G.17) becomes

$$\begin{aligned} \frac{\partial(E[y_{dc,R,n} y_{dc,R,n-k}])}{\partial(E[y_{R,n} y_{R,n-k}])} &= erf\left(\frac{A}{\sqrt{2\sigma_{yR,n}}}\right) erf\left(\frac{A}{\sqrt{2\sigma_{yR,n-k}}}\right) + \frac{4}{\pi} \sum_{m=2,4,\dots}^{\infty} \frac{r^m(n,k)}{2^m \cdot m!} \cdot \\ &\quad \int_0^{\frac{A}{\sqrt{2\sigma_{yR,n}}}} H_m(u) \exp(-u^2) du \cdot \int_0^{\frac{A}{\sqrt{2\sigma_{yR,n-k}}}} H_m(v) \exp(-v^2) dv. \end{aligned} \quad (\text{G.20})$$

To reduce (G.20), the integral $\int_0^{\frac{A}{\sqrt{2\sigma_{yR,n}}}} H_m(u) \exp(-u^2) du$ is the significant problem to resolve. According to the definition of $H_m(u)$ in (G.10), we are able to transform (G.20) into

$$\int_0^{\frac{A}{\sqrt{2\sigma_{yR,n}}}} H_m(u) \exp(-u^2) du = \int_0^{\frac{A}{\sqrt{2\sigma_{yR,n}}}} (-1)^m \frac{d^m}{du^m} \exp(-u^2) du, \quad (\text{G.21})$$

and let

$$h^{(m)}(u) \triangleq \frac{d^m}{du^m} \exp(-u^2), \quad (\text{G.22})$$

(G.21) then becomes

$$\begin{aligned} \int_0^{\frac{A}{\sqrt{2\sigma_{yR,n}}}} (-1)^m \frac{d^m}{du^m} \exp(-u^2) du &= \int_0^{\frac{A}{\sqrt{2\sigma_{yR,n}}}} (-1)^m h^{(m)}(u) du \\ &= (-1)^m \cdot [h^{(m-1)}(\frac{A}{\sqrt{2\sigma_{yR,n}}}) - h^{(m-1)}(0)] \end{aligned} \quad (\text{G.23})$$

Since $\exp(-u^2)$ is an even function, it is evident that $h^{(m-1)}(0) = 0$ if m is even, therefore,

$$\begin{aligned} \int_0^{\frac{A}{\sqrt{2\sigma_{yR,n}}}} H_m(u) \exp(-u^2) du &= (-1)^m \cdot h^{(m-1)}(\frac{A}{\sqrt{2\sigma_{yR,n}}}) \\ &= (-1)^m \cdot \frac{d^{m-1}}{du^{m-1}} \exp(-u^2) \Big|_{u=\frac{A}{\sqrt{2\sigma_{yR,n}}}}. \end{aligned} \quad (\text{G.24})$$

Again, according to the definition of Hermite polynomial in (G.10), we know that (G.21) can be converted into

$$\int_0^{\frac{A}{\sqrt{2\sigma_{yR,n}}}} H_m(u) \exp(-u^2) du = (-1) \cdot H_{m-1}(\frac{A}{\sqrt{2\sigma_{yR,n}}}) \exp(-\frac{A^2}{2\sigma_{yR,n}^2}). \quad (\text{G.25})$$

As a result, (G.8) becomes

$$\begin{aligned} \frac{\partial(E[y_{dc,R,n}y_{dc,R,n-k}])}{\partial(E[y_{R,n}y_{R,n-k}])} &= \operatorname{erf}(\frac{A}{\sqrt{2\sigma_{yR,n}}}) \operatorname{erf}(\frac{A}{\sqrt{2\sigma_{yR,n-k}}}) + \frac{4}{\pi} \sum_{m=2,4,\dots}^{\infty} \frac{r^m(n,k)}{2^m \cdot m!} \\ &\quad H_{m-1}(\frac{A}{\sqrt{2\sigma_{yR,n}}}) H_{m-1}(\frac{A}{\sqrt{2\sigma_{yR,n-k}}}) \cdot \exp(-\frac{A^2}{2\sigma_{yR,n}^2}) \exp(-\frac{A^2}{2\sigma_{yR,n-k}^2}). \end{aligned} \quad (\text{G.26})$$

Then we can derive $E[y_{dc,R,n}y_{dc,R,n-k}]$ by integrating on the both sides of (G.26),

it would be

$$\begin{aligned}
E[y_{dc,R}(n)y_{dc,R}(n-k)] &= \int_0^{E[y_{R,n}y_{R,n-k}]} \operatorname{erf}\left(\frac{A}{\sqrt{2}\sigma_{y_{R,n}}}\right)\operatorname{erf}\left(\frac{A}{\sqrt{2}\sigma_{y_{R,n-k}}}\right)dq \\
&+ \int_0^{E[y_{R,n}y_{R,n-k}]} \sum_{m=2,4,\dots}^{\infty} C_m q^m dq \\
&+ C_1
\end{aligned} \tag{G.27}$$

where

$$C_m = \frac{4H_{m-1}\left(\frac{A}{\sqrt{2}\sigma_{y_{R,n}}}\right)H_{m-1}\left(\frac{A}{\sqrt{2}\sigma_{y_{R,n-k}}}\right)}{\pi \cdot 2^m \cdot m! \cdot \sigma_{y_{R,n}}^m \cdot \sigma_{y_{R,n-k}}^m} \exp\left(-\frac{A^2}{2\sigma_{y_{R,n}}^2}\right) \exp\left(-\frac{A^2}{2\sigma_{y_{R,n-k}}^2}\right) \tag{G.28}$$

and C_1 is the constant to be determined.

Notice that we can determine C_1 from (G.3), (G.4) and (G.5). By letting $E[y_{R,n}y_{R,n-k}] = 0$ in (G.4), we have

$$\begin{aligned}
E[y_{dc,R}(n)y_{dc,R}(n-k)] &= \int_{-\infty}^{\infty} \int_{-\infty}^{\infty} g(y_{R,n})g(y_{R,n-k})f(y_{R,n}, y_{R,n-k})dy_{R,n}dy_{R,n-k} \\
&= \int_{-\infty}^{\infty} \int_{-\infty}^{\infty} g(y_{R,n})g(y_{R,n-k})f(y_{R,n})f(y_{R,n-k})dy_{R,n}dy_{R,n-k}.
\end{aligned} \tag{G.29}$$

According to the similar discussion in (E.7), we know that the above integral is 0, hence,

$$E[y_{dc,R}(n)y_{dc,R}(n-k)] = 0, \quad \text{if } E[y_{R,n}y_{R,n-k}] = 0, \tag{G.30}$$

(G.27) then becomes

$$\begin{aligned}
E[y_{dc,R}(n)y_{dc,R}(n-k)] &= \operatorname{erf}\left(\frac{A}{\sqrt{2}\sigma_{y_{R,n}}}\right)\operatorname{erf}\left(\frac{A}{\sqrt{2}\sigma_{y_{R,n-k}}}\right)E[y_{R,n}y_{R,n-k}] \\
&+ \sum_{m=2,4,\dots}^{\infty} D_m E^{m+1}[y_{R,n}y_{R,n-k}]
\end{aligned} \tag{G.31}$$

where

$$D_m = \frac{4H_{m-1}\left(\frac{A}{\sqrt{2}\sigma_{y_{R,n}}}\right)H_{m-1}\left(\frac{A}{\sqrt{2}\sigma_{y_{R,n-k}}}\right)}{\pi \cdot 2^m \cdot (m+1)! \cdot \sigma_{y_{R,n}}^m \cdot \sigma_{y_{R,n-k}}^m} \exp\left(-\frac{A^2}{2\sigma_{y_{R,n}}^2}\right) \exp\left(-\frac{A^2}{2\sigma_{y_{R,n-k}}^2}\right). \tag{G.32}$$

The above equation clearly shows the result of $E[y_{dc,R}(n)y_{dc,R}(n-k)]$.

What we wish to derive is the average autocorrelation of $y_{dc}(n)$, that is, $\sum_{n=0}^{M-1} E[y_{dc}(n)y_{dc}^*(n-k)]$. We know that second integral in (G.1) also has the similar analytical result as (G.31), hence

$$\begin{aligned}
E[y_{dc,I}(n)y_{dc,I}(n-k)] &= \operatorname{erf}\left(\frac{A}{\sqrt{2}\sigma_{y_{I,n}}}\right)\operatorname{erf}\left(\frac{A}{\sqrt{2}\sigma_{y_{I,n-k}}}\right)E[y_{I,n}y_{I,n-k}] \\
&+ \sum_{m=2,4,\dots}^{\infty} D_m E^{m+1}[y_{I,n}y_{I,n-k}]
\end{aligned} \tag{G.33}$$

and from the conclusion in (G.2), we are aware of that (G.31) and (G.33) are the same, that is,

$$E[y_{dc,R}(n)y_{dc,R}(n-k)] = E[y_{dc,I}(n)y_{dc,I}(n-k)]. \quad (\text{G.34})$$

Hence, by the conclusion shown in (G.1), $E[y_{dc}(n)y_{dc}^*(n-k)]$ results in

$$\begin{aligned} E[y_{dc}(n)y_{dc}^*(n-k)] &= \operatorname{erf}\left(\frac{A}{\sqrt{2}\sigma_{y_{R,n}}}\right)\operatorname{erf}\left(\frac{A}{\sqrt{2}\sigma_{y_{R,n-k}}}\right)E[y_n y_{n-k}^*] \\ &\quad + \sum_{m=2,4,\dots}^{\infty} D_m (E^{m+1}[y_{R,n}y_{R,n-k}] + E^{m+1}[y_{I,n}y_{I,n-k}]) \\ &= 2 \cdot \operatorname{erf}\left(\frac{A}{\sqrt{2}\sigma_{y_{R,n}}}\right)\operatorname{erf}\left(\frac{A}{\sqrt{2}\sigma_{y_{R,n-k}}}\right)E[y_{R,n}y_{R,n-k}] \\ &\quad + 2 \cdot \sum_{m=2,4,\dots}^{\infty} D_m E^{m+1}[y_{R,n}y_{R,n-k}], \end{aligned} \quad (\text{G.35})$$

and finally, the average autocorrelation of $y_{dc}(n)$, i.e., $\bar{R}_{y,dc}(k)$, can be derived as

$$\begin{aligned} \bar{R}_{y,dc}(k) &= \frac{2}{M} \sum_{n=0}^{M-1} \operatorname{erf}\left(\frac{A}{\sqrt{2}\sigma_{y_{R,n}}}\right)\operatorname{erf}\left(\frac{A}{\sqrt{2}\sigma_{y_{R,n-k}}}\right)E[y_{R,n}y_{R,n-k}] \\ &\quad + \frac{2}{M} \sum_{n=0}^{M-1} \sum_{m=2,4,\dots}^{\infty} D_m E^{m+1}[y_{R,n}y_{R,n-k}] \end{aligned} \quad (\text{G.36})$$

where D_m has been defined in (G.32).

Notice that from Lemma 5, when $w(n) = 1$, $0 \leq n < M - 1$, we have

$$\sigma_{y_{R,n}} = \sigma_{y_{R,n-k}} = \frac{1}{\sqrt{2}\sigma_x}, \quad \forall n, k \in \mathbb{Z} \quad (\text{G.37})$$

$$E[y_{R,n}y_{R,n-k}] = \sigma_x^2 \delta(k)$$

And (G.36) can be simplified as

$$\bar{R}_{y,dc}(k) = \frac{2}{M} \sigma_x^2 \operatorname{erf}^2\left(\frac{A}{\sigma_x}\right) \delta(k) + \frac{2}{M} \sum_{m=2,4,\dots}^{\infty} D_m \sigma_x^m \delta(k) \quad (\text{G.38})$$

where D_m can also be reduced as

$$D_m = \frac{4H_{m-1}^2\left(\frac{A}{\sigma_x}\right)}{\pi \cdot 2^m \cdot (m+1)! \cdot \sigma_x^{2m}} \cdot \exp\left(-\frac{A^2}{\sigma_x^2}\right). \quad (\text{G.39})$$

Appendix H

Proof of Lemma 16

Base on the conclusion of Lemma 15, we know that

$$\begin{aligned}
 E[y_{ac}(t)y_{ac}^*(t-\tau)] &= E[y_{ac,R}(t)y_{ac,R}(t-\tau)] + E[y_{ac,I}(t)y_{ac,I}(t-\tau)] \\
 &= \int_{-\infty}^{\infty} \int_{-\infty}^{\infty} g(y_{R,t})g(y_{R,t-\tau})f(y_{R,t}, y_{R,t-\tau})dy_{R,t}dy_{R,t-\tau} \\
 &\quad + \int_{-\infty}^{\infty} \int_{-\infty}^{\infty} g(y_{I,t})g(y_{I,t-\tau})f(y_{I,t}, y_{I,t-\tau})dy_{I,t}dy_{I,t-\tau}.
 \end{aligned} \tag{H.1}$$

Since $f(y_{R,t}, y_{R,t-\tau})$ and $f(y_{I,t}, y_{I,t-\tau})$ are both Gaussian distributed, and from (5.6), we have the relationship that

$$E[y_{R,t}y_{R,t-\tau}] = E[y_{I,t}y_{I,t-\tau}], \tag{H.2}$$

therefore, $f(y_{R,t}, y_{R,t-\tau}) = f(y_{I,t}, y_{I,t-\tau})$ and hence the following deduction can only focus on the first integral in (H.1), and the second integral can be derived in the similar manner.

We now emphasize the derivation of $E[y_{ac,R}(t)y_{ac,R}(t-\tau)]$, that is, to derive the closed form of

$$\int_{-\infty}^{\infty} \int_{-\infty}^{\infty} g(y_{R,t})g(y_{R,t-\tau})f(y_{R,t}, y_{R,t-\tau})dy_{R,t}dy_{R,t-\tau}. \tag{H.3}$$

The joint pdf of $f(y_{R,t}, y_{R,t-\tau})$ is

$$\begin{aligned}
 f(y_{R,t}, y_{R,t-\tau}) &= \frac{1}{2\pi\sigma_{y_{R,t}}\sigma_{y_{R,t-\tau}}\sqrt{1-r^2(t,\tau)}} \\
 &\quad \exp\left\{-\frac{1}{2(1-r^2(t,\tau))} \cdot \left(\frac{y_{R,t}^2}{\sigma_{y_{R,t}}^2} - 2r(t,\tau)\frac{y_{R,t}}{\sigma_{y_{R,t}}}\frac{y_{R,t-\tau}}{\sigma_{y_{R,t-\tau}}} + \frac{y_{R,t-\tau}^2}{\sigma_{y_{R,t-\tau}}^2}\right)\right\}
 \end{aligned} \tag{H.4}$$

where

$$r(t, \tau) = \frac{E[y_{R,t}y_{R,t-\tau}]}{\sigma_{y_{R,t}}\sigma_{y_{R,t-\tau}}} \quad (\text{H.5})$$

By Price's Theorem[18, 20]

$$\begin{aligned} \frac{\partial(E[y_{ac,R,t}y_{ac,R,t-\tau}])}{\partial(E[y_{R,t}y_{R,t-\tau}])} &= E\left\{\frac{\partial y_{ac,R,t}}{\partial y_{R,t}} \frac{\partial y_{ac,R,t-\tau}}{\partial y_{R,t-\tau}}\right\} \\ &= E\left\{\frac{\partial g(y_{R,t})}{\partial y_{R,t}} \frac{\partial g(y_{R,t-\tau})}{\partial y_{R,t-\tau}}\right\} \\ &= \int_{-\infty}^{\infty} \int_{-\infty}^{\infty} \frac{\partial g(y_{R,t})}{\partial y_{R,t}} \frac{\partial g(y_{R,t-\tau})}{\partial y_{R,t-\tau}} f(y_{R,t}, y_{R,t-\tau}) dy_{R,t} dy_{R,t-\tau}. \end{aligned} \quad (\text{H.6})$$

Due to the clipping function $g(\cdot)$, the intervals of the integrals can be divided into several regions, which lies on the linear and the nonlinear intervals of the clipping function. Thus, (H.6) becomes

$$\begin{aligned} \frac{\partial(E[y_{ac,R,t}y_{ac,R,t-\tau}])}{\partial(E[y_{R,t}y_{R,t-\tau}])} &= \int_{-A}^A \int_{-A}^A \frac{\partial y_{R,t}}{\partial y_{R,t}} \frac{\partial y_{R,t-\tau}}{\partial y_{R,t-\tau}} f(y_{R,t}, y_{R,t-\tau}) dy_{R,t} dy_{R,t-\tau} \\ &+ \int_{-A}^A \int_A^{\infty} \frac{\partial A}{\partial y_{R,t}} \frac{\partial y_{R,t-\tau}}{\partial y_{R,t-\tau}} f(y_{R,t}, y_{R,t-\tau}) dy_{R,t} dy_{R,t-\tau} \\ &+ \int_{-A}^A \int_{-\infty}^{-A} \frac{\partial(-A)}{\partial y_{R,t}} \frac{\partial y_{R,t-\tau}}{\partial y_{R,t-\tau}} f(y_{R,t}, y_{R,t-\tau}) dy_{R,t} dy_{R,t-\tau} \\ &+ \int_A^{\infty} \int_{-\infty}^{\infty} \frac{\partial g(y_{R,t})}{\partial y_{R,t}} \frac{\partial A}{\partial y_{R,t-\tau}} f(y_{R,t}, y_{R,t-\tau}) dy_{R,t} dy_{R,t-\tau} \\ &+ \int_{-\infty}^{-A} \int_{-\infty}^{\infty} \frac{\partial g(y_{R,t})}{\partial y_{R,t}} \frac{\partial(-A)}{\partial y_{R,t-\tau}} f(y_{R,t}, y_{R,t-\tau}) dy_{R,t} dy_{R,t-\tau}. \end{aligned} \quad (\text{H.7})$$

It is evident that all the integrals are zero except for the first one, therefore, only the first term is left in (H.7), that is,

$$\frac{\partial(E[y_{ac,R,t}y_{ac,R,t-\tau}])}{\partial(E[y_{R,t}y_{R,t-\tau}])} = \int_{-A}^A \int_{-A}^A f(y_{R,t}, y_{R,t-\tau}) dy_{R,t} dy_{R,t-\tau} \quad (\text{H.8})$$

By Mehler's formula [21], we know that

$$\frac{1}{\sqrt{1-\omega^2}} \exp\left(\frac{-\omega^2\alpha^2+2\omega\alpha\beta-\omega^2\beta^2}{1-\omega^2}\right) = \sum_{m=0}^{\infty} \frac{H_m(\alpha)H_m(\beta)\omega^m}{2^m \cdot m!} \quad (\text{H.9})$$

where $\alpha, \beta, \omega \in \mathbb{R}$ and $H_m(x)$ is the Hermite polynomial and defined as

$$H_m(x) = (-1)^m \exp(x^2) \frac{d^m}{dx^m} \exp(-x^2). \quad (\text{H.10})$$

Therefore, the joint pdf in (H.8) becomes

$$\begin{aligned}
f(y_{R,t}, y_{R,t-\tau}) &= \frac{1}{2\pi\sigma_{y_{R,t}}\sigma_{y_{R,t-\tau}}} \cdot \\
&\frac{1}{\sqrt{1-r^2(t,\tau)}} \exp\left\{\frac{-r^2(t,\tau)\left(\frac{y_{R,t}}{\sqrt{2}\sigma_{y_{R,t}}}\right)^2 + 2r(t,\tau)\left(\frac{y_{R,t}}{\sqrt{2}\sigma_{y_{R,t}}}\right)\left(\frac{y_{R,t-\tau}}{\sqrt{2}\sigma_{y_{R,t-\tau}}}\right) - r^2(t,\tau)\left(\frac{y_{R,t-\tau}}{\sqrt{2}\sigma_{y_{R,t-\tau}}}\right)^2}{1-r^2(t,\tau)}\right\} \cdot \\
&\exp\left\{\frac{(r^2(t,\tau)-1)\left(\frac{y_{R,t}}{\sqrt{2}\sigma_{y_{R,t}}}\right)^2}{1-r^2(t,\tau)}\right\} \cdot \exp\left\{\frac{(r^2(t,\tau)-1)\left(\frac{y_{R,t-\tau}}{\sqrt{2}\sigma_{y_{R,t-\tau}}}\right)^2}{1-r^2(t,\tau)}\right\} \\
&= \frac{1}{2\pi\sigma_{y_{R,t}}\sigma_{y_{R,t-\tau}}} \cdot \sum_{m=0}^{\infty} \frac{H_m\left(\frac{y_{R,t}}{\sqrt{2}\sigma_{y_{R,t}}}\right)H_m\left(\frac{y_{R,t-\tau}}{\sqrt{2}\sigma_{y_{R,t-\tau}}}\right)r^m(t,\tau)}{2^m \cdot m!} \cdot \\
&\exp\left\{-\left(\frac{y_{R,t}}{\sqrt{2}\sigma_{y_{R,t}}}\right)^2\right\} \cdot \exp\left\{-\left(\frac{y_{R,t-\tau}}{\sqrt{2}\sigma_{y_{R,t-\tau}}}\right)^2\right\},
\end{aligned} \tag{H.11}$$

and (H.8) can be simplified as

$$\begin{aligned}
\frac{\partial(E[y_{ac,R,t}y_{ac,R,t-\tau}])}{\partial(E[y_{R,t}y_{R,t-\tau}])} &= \frac{1}{2\pi\sigma_{y_{R,t}}\sigma_{y_{R,t-\tau}}} \sum_{m=0}^{\infty} \frac{r^m(t,\tau)}{2^m \cdot m!} \cdot \\
&\int_{-A}^A H_m\left(\frac{y_{R,t}}{\sqrt{2}\sigma_{y_{R,t}}}\right) \exp\left\{-\left(\frac{y_{R,t}}{\sqrt{2}\sigma_{y_{R,t}}}\right)^2\right\} dy_{R,t} \cdot \\
&\int_{-A}^A H_m\left(\frac{y_{R,t-\tau}}{\sqrt{2}\sigma_{y_{R,t-\tau}}}\right) \exp\left\{-\left(\frac{y_{R,t-\tau}}{\sqrt{2}\sigma_{y_{R,t-\tau}}}\right)^2\right\} dy_{R,t-\tau}.
\end{aligned} \tag{H.12}$$

Let $u = \frac{y_{R,t}}{\sqrt{2}\sigma_{y_{R,t}}}$, the first integral in (H.12) becomes

$$\int_{-A}^A H_m\left(\frac{y_{R,t}}{\sqrt{2}\sigma_{y_{R,t}}}\right) \exp\left\{-\left(\frac{y_{R,t}}{\sqrt{2}\sigma_{y_{R,t}}}\right)^2\right\} dy_{R,t} = \sqrt{2}\sigma_{y_{R,t}} \int_{-\frac{A}{\sqrt{2}\sigma_{y_{R,t}}}}^{\frac{A}{\sqrt{2}\sigma_{y_{R,t}}}} H_m(u) \exp(-u^2) du, \tag{H.13}$$

then, (H.12) turns into

$$\begin{aligned}
\frac{\partial(E[y_{ac,R,t}y_{ac,R,t-\tau}])}{\partial(E[y_{R,t}y_{R,t-\tau}])} &= \frac{1}{\pi} \sum_{m=0}^{\infty} \frac{r^m(t,\tau)}{2^m \cdot m!} \cdot \int_{-\frac{A}{\sqrt{2}\sigma_{y_{R,t}}}}^{\frac{A}{\sqrt{2}\sigma_{y_{R,t}}}} H_m(u) \exp(-u^2) du \cdot \\
&\int_{-\frac{A}{\sqrt{2}\sigma_{y_{R,t-\tau}}}}^{\frac{A}{\sqrt{2}\sigma_{y_{R,t-\tau}}}} H_m(v) \exp(-v^2) dv.
\end{aligned} \tag{H.14}$$

According to the definition of the Hermite polynomial $H_m(x)$ in (H.10), we know that

$$H_m(x) = \begin{cases} \text{even function,} & m \text{ is even} \\ \text{odd function,} & m \text{ is odd} \end{cases}. \quad (\text{H.15})$$

When m is odd, the integrand $H_m(u) \exp(-u^2)$ becomes an odd function. Due to the symmetry of the integral interval,

$$\begin{aligned} \int_{-\frac{A}{\sqrt{2\sigma_{y_{R,t}}}}}^{\frac{A}{\sqrt{2\sigma_{y_{R,t}}}}} H_m(u) \exp(-u^2) du &= 0, \text{ if } m \text{ is odd.} \\ \int_{-\frac{A}{\sqrt{2\sigma_{y_{R,t}}}}}^{\frac{A}{\sqrt{2\sigma_{y_{R,t}}}}} H_m(u) \exp(-u^2) du &= \int_0^{\frac{2A}{\sqrt{2\sigma_{y_{R,t}}}}} H_m(u) \exp(-u^2) du, \text{ if } m \text{ is even.} \end{aligned} \quad (\text{H.16})$$

Similar deduction process can be applied to the second integral in (H.14), then the further simplification of (H.14) can be derived as

$$\begin{aligned} \frac{\partial(E[y_{ac,R,t}y_{ac,R,t-\tau}])}{\partial(E[y_{R,t}y_{R,t-\tau}])} &= \frac{1}{\pi} \sum_{m=0,2,4,\dots}^{\infty} \frac{r^m(t,\tau)}{2^m \cdot m!} \cdot \int_{-\frac{A}{\sqrt{2\sigma_{y_{R,t}}}}}^{\frac{A}{\sqrt{2\sigma_{y_{R,t}}}}} H_m(u) \exp(-u^2) du \cdot \\ &\quad \int_{-\frac{A}{\sqrt{2\sigma_{y_{R,t-\tau}}}}}^{\frac{A}{\sqrt{2\sigma_{y_{R,t-\tau}}}}} H_m(v) \exp(-v^2) dv. \\ &= \frac{4}{\pi} \sum_{m=0,2,4,\dots}^{\infty} \frac{r^m(t,\tau)}{2^m \cdot m!} \cdot \int_0^{\frac{A}{\sqrt{2\sigma_{y_{R,t}}}}} H_m(u) \exp(-u^2) du \cdot \\ &\quad \int_0^{\frac{A}{\sqrt{2\sigma_{y_{R,t-\tau}}}}} H_m(v) \exp(-v^2) dv. \end{aligned} \quad (\text{H.17})$$

The $m = 0$ term is isolated now. Since the error function $\text{erf}(x)$ is defined as

$$\text{erf}(x) \triangleq \frac{2}{\sqrt{\pi}} \int_0^x \exp(-t^2) dt \quad (\text{H.18})$$

and

$$H_0(x) = 1, \quad \forall x \in \mathbb{R} \quad (\text{H.19})$$

(H.17) becomes

$$\begin{aligned} \frac{\partial(E[y_{ac,R,t}y_{ac,R,t-\tau}])}{\partial(E[y_{R,t}y_{R,t-\tau}])} &= \text{erf}\left(\frac{A}{\sqrt{2\sigma_{y_{R,t}}}}\right) \text{erf}\left(\frac{A}{\sqrt{2\sigma_{y_{R,t-\tau}}}}\right) + \frac{4}{\pi} \sum_{m=2,4,\dots}^{\infty} \frac{r^m(t,\tau)}{2^m \cdot m!} \cdot \\ &\quad \int_0^{\frac{A}{\sqrt{2\sigma_{y_{R,t}}}}} H_m(u) \exp(-u^2) du \cdot \int_0^{\frac{A}{\sqrt{2\sigma_{y_{R,t-\tau}}}}} H_m(v) \exp(-v^2) dv. \end{aligned} \quad (\text{H.20})$$

To reduce (H.20), the integral $\int_0^{\frac{A}{\sqrt{2\sigma_{yR,t}}}} H_m(u) \exp(-u^2) du$ is the significant problem to resolve. According to the definition of $H_m(u)$ in (H.10), we are able to transform (H.20) into

$$\int_0^{\frac{A}{\sqrt{2\sigma_{yR,t}}}} H_m(u) \exp(-u^2) du = \int_0^{\frac{A}{\sqrt{2\sigma_{yR,t}}}} (-1)^m \frac{d^m}{du^m} \exp(-u^2) du, \quad (\text{H.21})$$

and let

$$h^{(m)}(u) \triangleq \frac{d^m}{du^m} \exp(-u^2), \quad (\text{H.22})$$

(H.21) then becomes

$$\begin{aligned} \int_0^{\frac{A}{\sqrt{2\sigma_{yR,t}}}} (-1)^m \frac{d^m}{du^m} \exp(-u^2) du &= \int_0^{\frac{A}{\sqrt{2\sigma_{yR,t}}}} (-1)^m h^{(m)}(u) du \\ &= (-1)^m \cdot [h^{(m-1)}(\frac{A}{\sqrt{2\sigma_{yR,t}}}) - h^{(m-1)}(0)] \end{aligned} \quad (\text{H.23})$$

Since $\exp(-u^2)$ is an even function, it is evident that $h^{(m-1)}(0) = 0$ if m is even, therefore,

$$\begin{aligned} \int_0^{\frac{A}{\sqrt{2\sigma_{yR,t}}}} H_m(u) \exp(-u^2) du &= (-1)^m \cdot h^{(m-1)}(\frac{A}{\sqrt{2\sigma_{yR,t}}}) \\ &= (-1)^m \cdot \frac{d^{m-1}}{du^{m-1}} \exp(-u^2) \Big|_{u=\frac{A}{\sqrt{2\sigma_{yR,t}}}}. \end{aligned} \quad (\text{H.24})$$

Again, according to the definition of Hermite polynomial in (H.10), we know that (H.21) can be converted into

$$\int_0^{\frac{A}{\sqrt{2\sigma_{yR,t}}}} H_m(u) \exp(-u^2) du = (-1) \cdot H_{m-1}(\frac{A}{\sqrt{2\sigma_{yR,t}}}) \exp(-\frac{A^2}{2\sigma_{yR,t}^2}). \quad (\text{H.25})$$

As a result, (H.8) becomes

$$\begin{aligned} \frac{\partial(E[y_{ac,R,t}y_{ac,R,t-\tau}])}{\partial(E[y_{R,t}y_{R,t-\tau}])} &= \operatorname{erf}(\frac{A}{\sqrt{2\sigma_{yR,t}}}) \operatorname{erf}(\frac{A}{\sqrt{2\sigma_{yR,t-\tau}}}) + \frac{4}{\pi} \sum_{m=2,4,\dots}^{\infty} \frac{r^m(t,\tau)}{2^m \cdot m!} \\ &\quad H_{m-1}(\frac{A}{\sqrt{2\sigma_{yR,t}}}) H_{m-1}(\frac{A}{\sqrt{2\sigma_{yR,t-\tau}}}) \cdot \exp(-\frac{A^2}{2\sigma_{yR,t}^2}) \exp(-\frac{A^2}{2\sigma_{yR,t-\tau}^2}). \end{aligned} \quad (\text{H.26})$$

Then we can derive $E[y_{ac,R,t}y_{ac,R,t-\tau}]$ by integrating on the both sides of (H.26),

it would be

$$\begin{aligned}
E[y_{ac,R}(t)y_{ac,R}(t-\tau)] &= \int_0^{E[y_{R,t}y_{R,t-\tau}]} \operatorname{erf}\left(\frac{A}{\sqrt{2}\sigma_{y_{R,t}}}\right)\operatorname{erf}\left(\frac{A}{\sqrt{2}\sigma_{y_{R,t-\tau}}}\right)dq \\
&+ \int_0^{E[y_{R,t}y_{R,t-\tau}]} \sum_{m=2,4,\dots}^{\infty} C_m q^m dq \\
&+ C_1
\end{aligned} \tag{H.27}$$

where

$$C_m = \frac{4H_{m-1}\left(\frac{A}{\sqrt{2}\sigma_{y_{R,t}}}\right)H_{m-1}\left(\frac{A}{\sqrt{2}\sigma_{y_{R,t-\tau}}}\right)}{\pi \cdot 2^m \cdot m! \cdot \sigma_{y_{R,t}}^m \cdot \sigma_{y_{R,t-\tau}}^m} \exp\left(-\frac{A^2}{2\sigma_{y_{R,t}}^2}\right) \exp\left(-\frac{A^2}{2\sigma_{y_{R,t-\tau}}^2}\right) \tag{H.28}$$

and C_1 is the constant to be determined.

Notice that we can determine C_1 from (H.3), (H.4) and (H.5). By letting $E[y_{R,t}y_{R,t-\tau}] = 0$ in (H.4), we have

$$\begin{aligned}
E[y_{ac,R}(t)y_{ac,R}(t-\tau)] &= \int_{-\infty}^{\infty} \int_{-\infty}^{\infty} g(y_{R,t})g(y_{R,t-\tau})f(y_{R,t}, y_{R,t-\tau})dy_{R,t}dy_{R,t-\tau} \\
&= \int_{-\infty}^{\infty} \int_{-\infty}^{\infty} g(y_{R,t})g(y_{R,t-\tau})f(y_{R,t})f(y_{R,t-\tau})dy_{R,t}dy_{R,t-\tau}.
\end{aligned} \tag{H.29}$$

According to the similar discussion in (E.7), we know that the above integral is 0, hence,

$$E[y_{ac,R}(t)y_{ac,R}(t-\tau)] = 0, \quad \text{if } E[y_{R,t}y_{R,t-\tau}] = 0, \tag{H.30}$$

(H.27) then becomes

$$\begin{aligned}
E[y_{ac,R}(t)y_{ac,R}(t-\tau)] &= \operatorname{erf}\left(\frac{A}{\sqrt{2}\sigma_{y_{R,t}}}\right)\operatorname{erf}\left(\frac{A}{\sqrt{2}\sigma_{y_{R,t-\tau}}}\right)E[y_{R,t}y_{R,t-\tau}] \\
&+ \sum_{m=2,4,\dots}^{\infty} D_m E^{m+1}[y_{R,t}y_{R,t-\tau}]
\end{aligned} \tag{H.31}$$

where

$$D_m = \frac{4H_{m-1}\left(\frac{A}{\sqrt{2}\sigma_{y_{R,t}}}\right)H_{m-1}\left(\frac{A}{\sqrt{2}\sigma_{y_{R,t-\tau}}}\right)}{\pi \cdot 2^m \cdot (m+1)! \cdot \sigma_{y_{R,t}}^m \cdot \sigma_{y_{R,t-\tau}}^m} \exp\left(-\frac{A^2}{2\sigma_{y_{R,t}}^2}\right) \exp\left(-\frac{A^2}{2\sigma_{y_{R,t-\tau}}^2}\right). \tag{H.32}$$

The above equation clearly shows the result of $E[y_{ac,R}(t)y_{ac,R}(t-\tau)]$.

What we wish to derive is the average autocorrelation of $y_{ac}(t)$, that is,

$$\frac{1}{MT_s} \int_0^{MT_s} E[y_{ac}(t)y_{ac}^*(t-\tau)]dt.$$

We know that second integral in (H.1) also has the similar analytical result as (H.31), hence

$$\begin{aligned}
E[y_{ac,I}(t)y_{ac,I}(t-\tau)] &= \operatorname{erf}\left(\frac{A}{\sqrt{2}\sigma_{y_{I,t}}}\right)\operatorname{erf}\left(\frac{A}{\sqrt{2}\sigma_{y_{I,t-\tau}}}\right)E[y_{I,t}y_{I,t-\tau}] \\
&+ \sum_{m=2,4,\dots}^{\infty} D_m E^{m+1}[y_{I,t}y_{I,t-\tau}]
\end{aligned} \tag{H.33}$$

and from the conclusion in (H.2), we are aware of that (H.31) and (H.33) are the same, that is,

$$E[y_{ac,R}(t)y_{ac,R}(t-\tau)] = E[y_{ac,I}(t)y_{ac,I}(t-\tau)]. \tag{H.34}$$

Hence, by the conclusion shown in (H.1), $E[y_{ac}(t)y_{ac}^*(t-\tau)]$ results in

$$\begin{aligned}
E[y_{ac}(t)y_{ac}^*(t-\tau)] &= \operatorname{erf}\left(\frac{A}{\sqrt{2}\sigma_{y_{R,t}}}\right)\operatorname{erf}\left(\frac{A}{\sqrt{2}\sigma_{y_{R,t-\tau}}}\right)E[y_{R,t}y_{R,t-\tau}^*] \\
&+ \sum_{m=2,4,\dots}^{\infty} D_m (E^{m+1}[y_{R,t}y_{R,t-\tau}] + E^{m+1}[y_{I,t}y_{I,t-\tau}]) \\
&= 2 \cdot \operatorname{erf}\left(\frac{A}{\sqrt{2}\sigma_{y_{R,t}}}\right)\operatorname{erf}\left(\frac{A}{\sqrt{2}\sigma_{y_{R,t-\tau}}}\right)E[y_{R,t}y_{R,t-\tau}] \\
&+ 2 \cdot \sum_{m=2,4,\dots}^{\infty} D_m E^{m+1}[y_{R,t}y_{R,t-\tau}],
\end{aligned} \tag{H.35}$$

and finally, the average autocorrelation of $y_{ac}(t)$, i.e., $\overline{R}_{y,ac}(\tau)$, can be derived as

$$\begin{aligned}
\overline{R}_{y,ac}(\tau) &= \frac{2}{MT_s} \int_0^{MT_s} \operatorname{erf}\left(\frac{A}{\sqrt{2}\sigma_{y_{R,t}}}\right)\operatorname{erf}\left(\frac{A}{\sqrt{2}\sigma_{y_{R,t-\tau}}}\right)E[y_{R,t}y_{R,t-\tau}^*]dt \\
&+ \frac{2}{MT_s} \int_0^{MT_s} \sum_{m=2,4,\dots}^{\infty} D_m E^{m+1}[y_{R,t}y_{R,t-\tau}]dt
\end{aligned} \tag{H.36}$$

where D_m has been defined in (H.32).

Bibliography

- [1] R. W. Chang and R. A. Gibby, "A Theoretical Study of Performance of an Orthogonal Multiplexing Data Transmission Scheme," *IEEE Trans. Commun.*, vol. 16, no. 4, pp. 529-540, Aug. 1968.
- [2] L. J. Cimini Jr., "Analysis and Simulation of a Digital Mobile Channel using Orthogonal Frequency Division Multiplexing," *IEEE Trans. Commun.*, vol. 33, no. 7, pp. 665-675, July 1985.
- [3] J. A. C. Bingham, "Multicarrier Modulation for Data Transmission: An Idea Whose Time Has Come," *IEEE Commun. Mag.*, vol. 28, no. 5, pp. 5-14, May 1990.
- [4] "Special issue on multi-carrier communications", in *Wireless Personal Communications*, Amsterdam, The Netherlands: Kluwer Academic, vol. 2, no. 1, 1995.
- [5] G. L. Stuber, *Principles of Mobile Communication*, 2nd ed. Boston, MA: Kluwer, 2001.
- [6] *Asymmetric Digital Subscriber Lines (ADSL)-Metallic Interface*, ANSI T1.413, 1998.
- [7] *Very-high Speed Digital Subscriber Lines (VDSL)-Metallic Interface*, ANSI T1.424, 2002.
- [8] R. W. Bäuml, R. F. H. Fisher, and J. B. Huber, "Reducing the Peak-to-Average Power Ratio of Multicarrier Modulation by Selected Mapping," *Elect. Lett.*, vol. 32, no. 22, pp. 2056-2057, Oct. 1996.

- [9] S. H. Müller and J. B. Huber, "OFDM with Reduced Peak-to-Average Power Ratio by Optimum Combination of Partial Transmit Sequences," *Elect. Lett.*, vol. 33, no. 5, pp. 368-369 Feb. 1997.
- [10] R. O'Neill, L. Lopes, "Performance of Amplitude Limited Multitone Signals," *VTC 1994*, Vol. 3, pp.1675-1679, June 1994.
- [11] R. O'Neill and L. B. Lopes, "Envelope Variations and Spectral Splatter in Clipped Multicarrier Signals," in *Proc. IEEE PIMRC'95*, Toronto, Canada, pp. 71-75, Sept. 1995.
- [12] M. Friese, "OFDM signals with low crest-factor," in *Proc. IEEE GLOBECOM 97*, vol. 1, New York, NY, pp. 290-294, Nov. 1997.
- [13] H. Saeedi, M. Sharif, and F. Marvasti, "Clipping Noise Cancellation in OFDM Systems Using Oversampled Signal Reconstruction," *IEEE Commun. Lett.*, vol. 6, no. 2, pp. 73-75, Feb. 2002.
- [14] H. Chen and M. Haimovish, "Iterative Estimation and Cancellation of Clipping Noise for OFDM Signals," *IEEE Commun. Lett.*, vol. 7, no. 7, pp. 305-307, July 2003.
- [15] R. Dinis and A. Gusmao, "On the performance evaluation of OFDM transmission using clipping techniques," in *Proc. IEEE VTC 99 Fall*, Amsterdam, The Netherlands, pp. 2923-2928, Sept. 1999.
- [16] R. Gross and D. Veeneman, "SNR and spectral properties for a clipped DMT ADSL signal," in *Proc. VTC'94*, pp. 843-847, June 1994.
- [17] Y.-P. Lin and S.-M. Phoong, "OFDM transmitters: analog representation and DFT-based implementation," *IEEE Trans. Signal Process.*, vol. 51, no. 9, pp. 2450-2453, Sep. 2003.
- [18] A. Papoulis, *Probability, Random Variables, and Stochastic Processes*, New York, McGraw-Hill, 1965.
- [19] John G. Proakis, *Digital Communications*, McGraw-Hill, Fourth. Edition, 2001.

- [20] R. Price, "A Useful Theorem for Nonlinear Devices Having Gaussian Inputs," *I.R.E. Trans. Inform. Theory*, IT-4, pp. 69-72, Jun. 1958.
- [21] G. Szego, *Orthogonal Polynomials*, New York, American Mathematical Society, 1959.
- [22] A. V. Oppenheim and R. W. Schaffer, *Discrete-Time Signal Processing*, Prentice-Hall, Englewood Cliffs, New Jersey, 1989.

